

# Properties of Excited Charm and Charm-Strange Mesons

Stephen Godfrey\* and Kenneth Moats

Ottawa-Carleton Institute for Physics, Department of Physics,  
Carleton University, Ottawa, Canada K1S 5B6

(Dated: January 15, 2016)

We calculate the properties of excited charm and charm-strange mesons. We use the relativized quark model to calculate their masses and wavefunctions that are used to calculate radiative transition partial widths and the  $^3P_0$  quark-pair-creation model to calculate their strong decay widths. We use these results to make quark model spectroscopic assignments for recently observed charm and charm-strange mesons. In particular we find that the properties of the  $D_J(2550)^0$  and  $D_J^*(2600)^0$  are consistent with those of the  $2^1S_0(c\bar{u})$  and the  $2^3S_1(c\bar{u})$  states respectively, the  $D_1^*(2760)^0$ ,  $D_3^*(2760)^-$ , and  $D_J(2750)^0$  with those of the  $1^3D_1(c\bar{u})$ ,  $1^3D_3(d\bar{c})$ , and  $1D_2(c\bar{u})$  states respectively. We tentatively identify the  $D_J^*(3000)^0$  as the  $1^3F_4(c\bar{u})$  and favour the  $D_J(3000)^0$  to be the  $3^1S_0(c\bar{u})$  although we do not rule out the  $1F_3$  and  $1F_3'$  assignment. For the recently observed charm-strange mesons we identify the  $D_{s1}^*(2709)^\pm$ ,  $D_{s1}^*(2860)^-$ , and  $D_{s3}^*(2860)^-$  as the  $2^3S_1(c\bar{s})$ ,  $1^3D_1(s\bar{c})$ , and  $1^3D_3(s\bar{c})$  states respectively and suggest that the  $D_{sJ}(3044)^\pm$  is most likely the  $D_{s1}(2P_1')$  or  $D_{s1}(2P_1)$  states although it might be the  $D_{s2}^*(2^3P_2)$  with the  $DK$  final state too small to be observed with current statistics. Based on the predicted properties of excited states, that they not have too large a total width and they have a reasonable branching ratio to simple final states, we suggest states that should be able to be found in the near future. We expect that the tables of properties summarizing our results will be useful for interpreting future observations of charm and charm-strange mesons.

PACS numbers: 12.39.Pn, 13.25.-k, 13.25.Ft, 14.40.Lb

## I. INTRODUCTION

Over the last decade, charm meson spectroscopy has undergone a resurgence due to the discovery of numerous excited charm and charm-strange states by the  $B$ -Factory experiments BaBar and Belle [1–7] and by the CLEO experiment [8]. More recently the LHCb experiment has demonstrated the capability of both observing these states and determining their properties [9–14]. This has led to considerable theoretical interest in attempting to make quark model spectroscopic assignments for these new states by comparing theoretical predictions to experimental measurements [15–32]. At the same time, steady progress is being made in lattice QCD [33–35] for which these experimental results and spectroscopic classifications are an important benchmark. With the start of higher energy and higher luminosity beams at the LHC and higher luminosity at the SuperKEKB  $e^+e^-$  collider we expect that more new states will be observed. To identify newly discovered states, a theoretical roadmap is needed. The quark model has been successful in taking on this role and we turn to it to calculate the properties of excited charm and charm-strange mesons.

An important property of heavy-light mesons is that in the limit that the heavy quark mass becomes infinite the properties of the meson are determined by those of the light quark [36–38]. The light quarks are characterized by their total angular momentum  $j_q$  such that

$\vec{j}_q = \vec{s}_q + \vec{L}$  where  $s_q$  is the light quark spin and  $L$  is its orbital angular momentum.  $j_q$  is combined with  $S_Q$ , the spin of the heavy quark, to give the total angular momentum of the meson. The quantum numbers  $S_Q$  and  $j_q$  are separately conserved. Thus, for a given  $L$ , the states will be grouped into doublets characterized by the angular momentum of the light quark. For example, the four  $L = 1$   $P$ -wave mesons can be grouped into two doublets characterized by the angular momentum of the light quark  $j_q = 3/2$  with  $J^P = 1^+, 2^+$  and  $j_q = 1/2$  with  $J^P = 0^+, 1^+$  where  $J$  and  $P$  are the total angular momentum and parity of the excited meson. In the heavy quark limit (HQL) the members of the doublets will be degenerate in mass, and this degeneracy is broken by  $1/m_Q$  corrections [38, 39]. For the  $L = 1$  multiplet, heavy quark symmetry and conservation of parity and  $j_q$  also predict that the strong decays  $D_{(s)J}^{(*)}(j_q = 3/2) \rightarrow D^{(*)}\pi(K)$  will only proceed through a  $D$ -wave while the decays  $D_{(s)J}^{(*)}(j_q = 1/2) \rightarrow D^{(*)}\pi(K)$  will only proceed via an  $S$ -wave [40, 41]. The states decaying to a  $D$ -wave are expected to be narrow due to the angular momentum barrier while those decaying to an  $S$ -wave are expected to be broad. Similar patterns are predicted for higher  $L$  multiplets so that measuring the properties of excited charm mesons can be used to both help identify them and to see how well excited states are described by the properties expected in the heavy quark limit. However, for higher mass states more phase space is available, leading to more possible decay channels, resulting in more complicated decay patterns so that the predictions of the HQL are less apparent.

Our goals for this paper are twofold. First we want to

\*Email: godfrey@physics.carleton.ca

provide a roadmap of charm and charm-strange meson properties to identify which states are the most promising candidates to be observed and the final states they are most likely to be observed in. Hereafter, for conciseness, we will generally refer to both charm and charm-strange mesons as charm mesons. Second, when new states are observed we can use our roadmap to make quark model spectroscopic assignments for these newly found states.

In the first part of this paper we calculate the masses and wavefunctions of excited charm and charm-strange mesons using the relativized quark model [42] which we describe in the next section. Radiative transitions are described in Section III and strong decay widths are calculated using the  ${}^3P_0$  quark-pair creation model [43, 44] which is described in Section IV. These models have been described extensively in the literature so rather than repeating detailed descriptions of these models we will give brief summaries and refer the interested reader to the references for further details. The outcome of this part of the paper is a comprehensive summary of excited charm meson properties.

In the second part, in Sections V and VI, we use these results to examine the numerous newly observed charm and charm-strange mesons and attempt to make quark model spectroscopic assignments. This approach has been used in numerous papers although in some cases different calculations come to different conclusions. Thus, another goal of this paper is to suggest further diagnostic measurements that can resolve these differences to give an unambiguous spectroscopic assignment. In Section VII we will use the quark model roadmap we produced in the first part of this paper to suggest which missing states, because of their properties, are most likely to be observed in the near future and suggest the most promising final states to study. We summarize our conclusions in the final section.

## II. SPECTROSCOPY

We use the relativized quark model [42] (see also Ref. [45–48]) to calculate meson masses and their wavefunctions which we use to calculate decay properties. The model is described in detail in Ref. [42] to which we direct the interested reader. The general characteristics of this model are that it assumes a relativistic kinetic energy term and the potential incorporates a Lorentz vector one-gluon-exchange interaction with a QCD motivated running coupling constant,  $\alpha_s(r)$ , and a Lorentz scalar linear confining interaction. This is typical of most such models which are based on some variant of the Coulomb plus linear potential expected from QCD and that often include some relativistic effects [20, 49–55]. The relativized quark model has been reasonably successful in describing most known mesons and has proven to be a useful guide to understanding newly found states [31, 41, 56–59]. However in recent years, starting with the discovery of the  $D_{sJ}(2317)$  [8, 60, 61] and  $X(3872)$  states [62], an

increasing number of states have been observed that do not fit into this picture [63–66] pointing to the need to include physics which has hitherto been neglected such as coupled channel effects [67] which appears to be most important for states lying near kinematic thresholds. As a consequence of neglecting coupled channel effects and the crudeness of the relativization procedure we do not expect the mass predictions to be accurate to better than  $\sim 10 - 20$  MeV.

For the case of a quark and antiquark of unequal mass, charge conjugation parity is no longer a good quantum number so that states with different total spins but with the same total angular momentum, such as the  ${}^3P_1 - {}^1P_1$  and  ${}^3D_2 - {}^1D_2$  pairs, can mix via the spin orbit interaction or some other mechanism. Consequently, the physical  $J = 1$   $P$ -wave states are linear combinations of  ${}^3P_1$  and  ${}^1P_1$  which we describe by:

$$\begin{aligned} P &= {}^1P_1 \cos \theta_{nP} + {}^3P_1 \sin \theta_{nP} \\ P' &= -{}^1P_1 \sin \theta_{nP} + {}^3P_1 \cos \theta_{nP} \end{aligned} \quad (1)$$

where  $P \equiv L = 1$  designates the relative angular momentum of the  $c\bar{q}$  pair and the subscript  $J = 1$  is the total angular momentum of the  $c\bar{q}$  pair which is equal to  $L$ , and  $q$  can represent either a  $u$ ,  $d$  or  $s$  quark. There are analogous expressions for higher  $L$  states where  $L = D, F$ , etc. Our notation implicitly implies  $L - S$  coupling between the quark spins and the relative orbital angular momentum. In the heavy quark limit in which the heavy quark mass  $m_Q \rightarrow \infty$ , the states can be described by the total angular momentum of the light quark,  $j_q$ , which couples to the spin of the heavy quark and corresponds to  $j - j$  coupling. In this limit the mixed states are given by [68]

$$\begin{aligned} |J = L, j_q = L + \frac{1}{2}\rangle &= \sqrt{\frac{J+1}{2J+1}} |J = L, S = 0\rangle \\ &\quad + \sqrt{\frac{J}{2J+1}} |J = L, S = 1\rangle \\ |J = L, j_q = L - \frac{1}{2}\rangle &= -\sqrt{\frac{J}{2J+1}} |J = L, S = 0\rangle \\ &\quad + \sqrt{\frac{J+1}{2J+1}} |J = L, S = 1\rangle \end{aligned} \quad (2)$$

The  $j_q = L - \frac{1}{2}$  state that is mainly spin triplet corresponds to the primed state in eqn. 1 and the  $j_q = L + \frac{1}{2}$  that is mainly spin singlet corresponds to the unprimed state. For  $L = 1$  the HQL gives rise to two doublets, one with  $j_q = 1/2$  and the other with  $j_q = 3/2$  and with the conventions of eqns. 1 and 2 corresponds to  $\theta_P = \tan^{-1}(-1/\sqrt{2}) \simeq -35.3^\circ$ . For  $L = 2$  the HQL gives two doublets with  $j_q = 3/2$  and  $5/2$  with mixing angle  $\theta_D = -\tan^{-1}(\sqrt{2/3}) = -39.2^\circ$ . The minus signs arise from our  $c\bar{q}$  convention. Some authors prefer to use the  $j - j$  basis [69] but since we solve our Hamiltonian equations assuming  $L - S$  eigenstates and then include the  $LS$  mixing we use the notation of eqn. 1. Radiative transitions are sensitive to the  ${}^3L_L - {}^1L_L$  mixing

angle. We note that the definition of the mixing angles are fraught with ambiguities. For example, charge conjugating  $c\bar{q}$  into  $q\bar{c}$  flips the sign of the angle and the phase convention depends on the order of coupling  $\vec{L}$ ,  $\vec{S}_q$  and  $\vec{S}_{\bar{q}}$  [70].

To solve the Hamiltonian to obtain masses and wavefunctions we used the following parameters: the slope of the linear confining potential is  $0.18 \text{ GeV}^2$ ,  $m_q = 0.22 \text{ GeV}$ ,  $m_s = 0.419 \text{ GeV}$  and  $m_c = 1.628 \text{ GeV}$ . The predictions of our model for the charm mesons are given in Fig. 1 and for the charm-strange mesons in Fig 2 and the predicted masses and  ${}^3L_L - {}^1L_L$  mixing angles are given in Tables I and II.

TABLE I: Predicted charm and charm-strange  $S$  and  $P$ -wave meson masses, spin-orbit mixing angles and  $\beta_{eff}$ 's. The  $P_1 - P_1'$  states and mixing angles are defined using the convention of eqn. 1. Where two values of  $\beta_{eff}$  are listed, the first value is for the singlet state and the second value is for the triplet state.

State	$c\bar{q}$		$c\bar{s}$	
	Mass	$\beta_{eff}$	Mass	$\beta_{eff}$
$1^3S_1$	2041	0.516	2129	0.562
$1^1S_0$	1877	0.601	1979	0.651
$2^3S_1$	2643	0.434	2732	0.458
$2^1S_0$	2581	0.450	2673	0.475
$3^3S_1$	3110	0.399	3193	0.415
$3^1S_0$	3068	0.407	3154	0.424
$4^3S_1$	3497	0.382	3575	0.393
$4^1S_0$	3468	0.387	3547	0.400
$5^3S_1$	3837	0.371	3912	0.383
$5^1S_0$	3814	0.376	3894	0.393
$1^3P_2$	2502	0.437	2592	0.464
$1P_1$	2456	0.475, 0.482	2549	0.498, 0.505
$1P_1'$	2467	0.475, 0.482	2556	0.498, 0.505
$1^3P_0$	2399	0.516	2484	0.542
$\theta_{1P}$	$-25.68^\circ$		$-37.48^\circ$	
$2^3P_2$	2957	0.402	3048	0.420
$2P_1$	2924	0.417, 0.419	3018	0.433, 0.434
$2P_1'$	2961	0.417, 0.419	3038	0.433, 0.434
$2^3P_0$	2931	0.431	3005	0.444
$\theta_{2P}$	$-29.39^\circ$		$-30.40^\circ$	
$3^3P_2$	3353	0.383	3439	0.396
$3P_1$	3328	0.392, 0.392	3416	0.404, 0.404
$3P_1'$	3360	0.392, 0.392	3433	0.404, 0.404
$3^3P_0$	3343	0.398	3412	0.409
$\theta_{3P}$	$-28.10^\circ$		$-27.72^\circ$	
$4^3P_2$	3701	0.371	3783	0.382
$4P_1$	3681	0.378, 0.377	3764	0.387, 0.387
$4P_1'$	3709	0.378, 0.377	3778	0.387, 0.387
$4^3P_0$	3697	0.381	3764	0.390
$\theta_{4P}$	$-26.91^\circ$		$-25.43^\circ$	

TABLE II: Predicted charm and charm-strange  $D$ ,  $F$ , and  $G$ -wave meson masses, spin-orbit mixing angles and  $\beta_{eff}$ 's. The  $D_2 - D_2'$ ,  $F_3 - F_3'$  and  $G_4 - G_4'$  states and mixing angles are defined using the convention of eqn. 1. Where two values of  $\beta_{eff}$  are listed, the first value is for the singlet state and the second value is for the triplet state.

State	$c\bar{q}$		$c\bar{s}$	
	Mass	$\beta_{eff}$	Mass	$\beta_{eff}$
$1^3D_3$	2833	0.407	2917	0.426
$1D_2$	2816	0.428, 0.433	2900	0.444, 0.448
$1D_2'$	2845	0.428, 0.433	2926	0.444, 0.448
$1^3D_1$	2817	0.456	2899	0.469
$\theta_{1D}$	$-38.17^\circ$		$-38.47^\circ$	
$2^3D_3$	3226	0.385	3311	0.400
$2D_2$	3212	0.396, 0.399	3298	0.408, 0.410
$2D_2'$	3248	0.396, 0.399	3323	0.408, 0.410
$2^3D_1$	3231	0.410	3306	0.419
$\theta_{2D}$	$-37.44^\circ$		$-37.71^\circ$	
$3^3D_3$	3579	0.372	3661	0.383
$3D_2$	3566	0.379, 0.381	3650	0.389, 0.390
$3D_2'$	3600	0.379, 0.381	3672	0.389, 0.390
$3^3D_1$	3588	0.387	3658	0.395
$\theta_{3D}$	$-36.90^\circ$		$-37.15^\circ$	
$1^3F_4$	3113	0.390	3190	0.405
$1F_3$	3108	0.404, 0.407	3186	0.417, 0.419
$1F_3'$	3143	0.404, 0.407	3218	0.417, 0.419
$1^3F_2$	3132	0.423	3208	0.432
$\theta_{1F}$	$-39.52^\circ$		$-39.30^\circ$	
$2^3F_4$	3466	0.374	3544	0.386
$2F_3$	3461	0.383, 0.385	3540	0.393, 0.394
$2F_3'$	3498	0.383, 0.385	3569	0.393, 0.394
$2^3F_2$	3490	0.394	3562	0.401
$\theta_{2F}$	$-39.38^\circ$		$-39.12^\circ$	
$1^3G_5$	3362	0.379	3433	0.391
$1G_4$	3364	0.389, 0.391	3436	0.399, 0.401
$1G_4'$	3399	0.389, 0.391	3469	0.399, 0.401
$1^3G_3$	3397	0.402	3469	0.410
$\theta_{1G}$	$-40.18^\circ$		$-39.95^\circ$	
$2^3G_5$	3685	0.367	3757	0.377
$2G_4$	3686	0.374, 0.375	3759	0.382, 0.383
$2G_4'$	3722	0.374, 0.375	3790	0.382, 0.383
$2^3G_3$	3721	0.383	3789	0.389
$\theta_{2G}$	$-40.23^\circ$		$-39.93^\circ$	

### III. RADIATIVE TRANSITIONS

Radiative transitions have the potential to give information that could help identify newly discovered states. They are sensitive to the internal structure of states and can be particularly sensitive to  ${}^3L_L - {}^1L_L$  mixing for states with  $J = L$ . However, in general, charm mesons lie above the OZI decay threshold so will have much larger

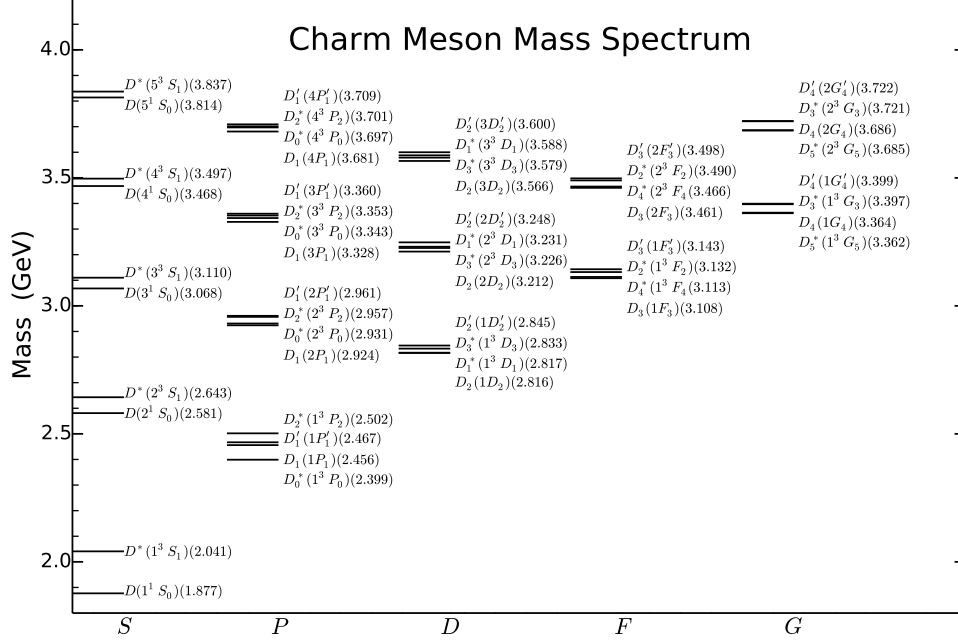


FIG. 1: The charm meson mass spectrum as predicted by the relativized quark model [42]. The  ${}^3L_L - {}^1L_L$  mixing angles are given in Tables I and II.

strong decay partial widths than electromagnetic partial widths so in practice we expect the usefulness of electromagnetic transitions to be limited. Nevertheless, in

this section we calculate E1 and M1 radiative widths. The partial width for an E1 radiative transition between states in the nonrelativistic quark model is given by [71]

$$\Gamma(n^{2S+1}L_J \rightarrow n'^{2S'+1}L'_{J'} + \gamma) = \frac{4}{3} \langle e_Q \rangle^2 \alpha k_\gamma^3 C_{fi} \delta_{SS'} \delta_{LL' \pm 1} |\langle n'^{2S'+1}L'_{J'} | r | n^{2S+1}L_J \rangle|^2, \quad (3)$$

where

$$\langle e_Q \rangle = \frac{m_c e_q - m_q e_{\bar{c}}}{m_q + m_c} \quad (4)$$

$e_c = 2/3$  is the  $c$ -quark charge and  $q$  refers to the  $u$ ,  $d$  and  $s$ -quarks with charges  $e_u = 2/3$ ,  $e_d = -1/3$  and  $e_s = -1/3$  respectively, in units of  $|e|$ ,  $\alpha$  is the fine-structure constant,  $k_\gamma$  is the photon's energy, and the angular momentum matrix element,  $C_{fi}$ , is given by

$$C_{fi} = \max(L, L')(2J' + 1) \left\{ \begin{matrix} L' & J' & S \\ J & L & 1 \end{matrix} \right\}^2 \quad (5)$$

where  $\left\{ \dots \right\}$  is a 6- $j$  symbol. The matrix elements  $\langle n'^{2S'+1}L'_{J'} | r | n^{2S+1}L_J \rangle$  were evaluated using the wave-

functions given by the relativized quark model [42]. Relativistic corrections are implicitly included in these E1 transitions through Siegert's theorem [72–74], by including spin-dependent interactions in the Hamiltonian used to calculate the meson masses and wavefunctions.

Radiative transitions which flip spin are described by magnetic dipole (M1) transitions. The rates for magnetic dipole transitions between  $S$ -wave states in heavy-light bound states are given in the nonrelativistic approximation by [75–77]

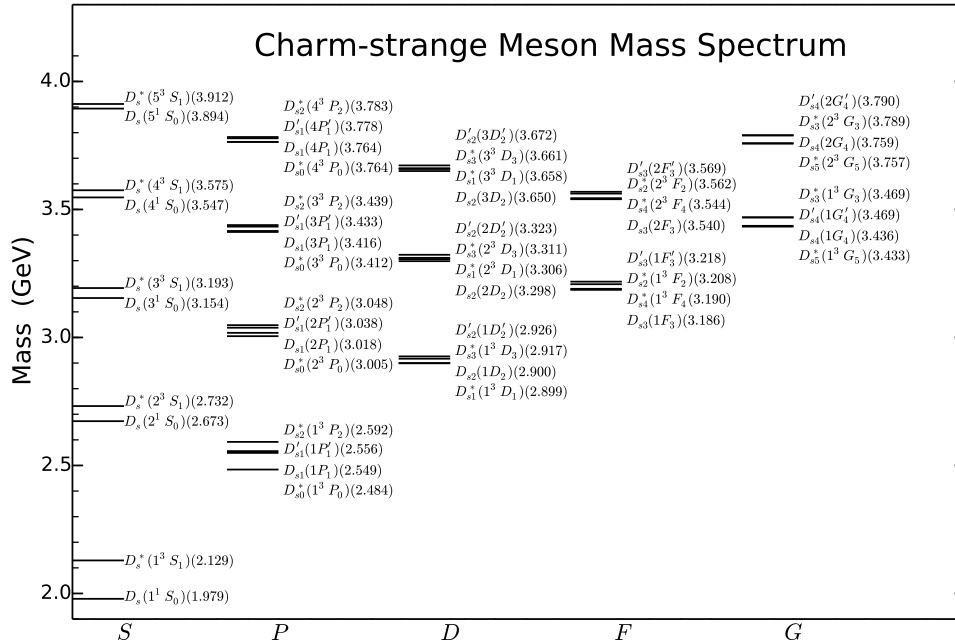


FIG. 2: The charm-strange meson mass spectrum as predicted by the relativized quark model [42]. The  ${}^3L_L - {}^1L_L$  mixing angles are given in Tables I and II.

$$\Gamma(n^{2S+1}L_J \rightarrow n'^{2S'+1}L_{J'} + \gamma) = \frac{\alpha}{3} k_\gamma^3 (2J' + 1) \delta_{S,S' \pm 1} |\langle f | \frac{e_q}{m_q} j_0(k_\gamma r \frac{m_{\bar{q}}}{m_q + m_{\bar{q}}}) - \frac{e_{\bar{q}}}{m_{\bar{q}}} j_0(k_\gamma r \frac{m_q}{m_q + m_{\bar{q}}}) | i \rangle|^2 \quad (6)$$

where  $e_q$ , the quark charges, and  $m_q$ , the quark masses were given above,  $L = 0$  for  $S$ -waves and  $j_0(x)$  is the spherical Bessel function. Transitions in which the principle quantum number changes are referred to as hindered transitions as they are not allowed in the non-relativistic limit due to the orthogonality of the wavefunctions. M1 transitions, especially hindered transitions, are notorious for their sensitivity to relativistic corrections [78]. In our calculations the wavefunction orthogonality is broken by including a smeared hyperfine interaction directly in the Hamiltonian so that the  ${}^3S_1$  and  ${}^1S_0$  states have slightly different wavefunctions.

The E1 and M1 radiative widths are given in Tables IV–XXVIII when they are large enough that they might be observed. More complete results are given in the supplementary material. The tables in the supplementary material also include the matrix elements for the benefit of the interested reader. The predicted masses given in Tables I and II are used for all states. The photon energies were calculated using the predicted masses, but assuming these masses are all slightly shifted with respect

to the measured masses, the phase space should remain approximately correct.

Given the sensitivity of radiative transitions to details of the models precise measurements of electromagnetic transition rates would provide stringent tests of the various calculations and predictions that have appeared in the literature.

#### IV. STRONG DECAYS

For states above the  $D\pi$  and  $DK$  thresholds we calculate the strong decay widths of excited charm and charm-strange mesons using the  ${}^3P_0$  quark pair creation model [43, 44, 57, 58, 79]. There are a number of predictions for charm meson widths in the literature using the  ${}^3P_0$  model [19–24, 55, 80, 81] and other models [15–17, 39, 49, 82–84] but we believe that this work represents the most complete analysis of excited charm meson strong decays to date. The details of the notation and conventions used in our  ${}^3P_0$  model calculations are given in the Appendix

TABLE III: Light meson masses and effective harmonic oscillator parameters,  $\beta_{eff}$ , used in the calculation of strong decay widths. The experimental values of the masses are taken from the Particle Data Group (PDG) [7]. The input value of the  $\pi$  mass is the weighted average of the experimental values of the  $\pi^0$  and  $\pi^\pm$  masses, and similarly for the input values of the  $K$  and  $K^*$  masses. All effective  $\beta$  values are taken to be 0.4 for the light mesons.

Meson	State	$M_{input}$ (MeV)	$M_{exp}$ (MeV) [7]	$\beta_{eff}$ (GeV)
$\pi$	$1^1S_0$	138.8877	$134.8766 \pm 0.0006$ ( $\pi^0$ ), $139.57018 \pm 0.00035$ ( $\pi^\pm$ )	0.4
$\eta$	$1^1S_0$	547.862	$547.862 \pm 0.018$	0.4
$\eta'$	$1^1S_0$	957.78	$957.78 \pm 0.06$	0.4
$\rho$	$1^3S_1$	775.26	$775.26 \pm 0.25$	0.4
$\omega$	$1^3S_1$	782.65	$782.65 \pm 0.12$	0.4
$\phi$	$1^3S_1$	1019.461	$1019.461 \pm 0.019$	0.4
$K$	$1^1S_0$	494.888	$497.614 \pm 0.024$ ( $K^0$ ), $493.677 \pm 0.016$ ( $K^\pm$ )	0.4
$K^*$	$1^3S_1$	894.36	$895.81 \pm 0.19$ ( $K^{*0}$ ), $891.66 \pm 0.26$ ( $K^{*\pm}$ )	0.4

of Ref. [85] to which we refer the interested reader.

We use the calculated charm and charm-strange meson masses listed in Tables I and II. For the light mesons we used the measured masses listed in Table III. For the charm and charm-strange mesons we use harmonic oscillator (HO) wave functions with the effective harmonic oscillator parameter,  $\beta_{eff}$ , obtained by equating the rms radius of the harmonic oscillator wavefunction for the specified  $(n, l)$  quantum numbers to the rms radius of the wavefunctions calculated using the relativized quark model of Ref. [42]. A previous study [41] found that using HO wavefunctions with the fitted oscillator parameters gave results similar to those calculated using the exact relativized quark model wavefunctions but were far more computationally efficient. It was also found that the predictions of the  $^3P_0$  model were similar to those of the flux-tube breaking model [86] when using the same wavefunctions in both calculations [41, 58, 87]. The widest variation in results occurs going from using either the exact relativized quark model wavefunctions or HO wavefunctions with  $\beta_{eff}$ 's to using constant  $\beta$ 's for all states [41] (compare also the results from Ref. [85] to those of Ref. [88]). This is because the decay amplitudes are dominated by the overlap of the three meson wavefunctions and the HO wavefunctions with  $\beta_{eff}$ 's are a good representation of the exact wavefunctions for this purpose. The effective harmonic oscillator wavefunction parameters,  $\beta_{eff}$ , used in our calculations are listed in Tables I and II. For the light mesons we use the universal value of  $\beta_{eff} = 0.4$  GeV given in Table III (see below for an additional comment). In our calculations we use the constituent quark masses  $m_c = 1.628$  GeV,  $m_s = 0.419$  GeV, and  $m_q = 0.220$  GeV ( $q = u, d$ ). Finally, we use “relativistic phase space” as described in Ref. [58, 79] and in the Appendix of Ref. [85].

Typical values of the parameters  $\beta_{eff}$  and  $\gamma$ , the quark pair creation amplitude of the  $^3P_0$  model, are found from fits to light meson decays [55, 58]. The predicted widths are fairly insensitive to the precise values used for  $\beta_{eff}$  provided  $\gamma$  is appropriately rescaled. However  $\gamma$  can vary as much as 30% and still give reasonable overall fits of

light meson decay widths [55]. This can result in factor of two changes to predicted widths, both smaller or larger. In our calculations of  $D_s$  meson strong decay widths in [31], we used a value of  $\gamma = 0.4$ , which has also been found to give a good description of strong decays of charmonium [55, 57]. This scaling of the value of  $\gamma$  in different meson sectors has been studied in [89]. The resulting strong decay widths are listed in Tables IV-XLIII although we only show decays that have branching ratios greater than  $\sim 1\%$  or decays to simple final states such as  $D\pi$  or  $DK$  that might be easier to observe. More complete tables of results are given in the supplementary material.

TABLE IV: Partial widths and branching ratios for strong and electromagnetic decays for the  $1S$ ,  $2S$  and  $3S$  charm mesons. The initial state's mass is given in GeV and is listed below the state's name in column 1. We only show radiative transitions that are likely to be observed and likewise generally do not show strong decay modes which have  $\text{BR} \lesssim 1\%$  although they are included in calculating the total width and are included in the supplementary material. The matrix elements for radiative transitions are given in the supplementary material. Details of the calculations are given in the text.

Initial state	Final state	Width ( $cu, cd$ ) (MeV)	B.R. ( $cu, cd$ ) (%)	
$D^*$ 2041	$D\gamma$	0.106, 0.0108	45.9, 8.0	
	$D\pi$	0.125	54.1, 92.1	
	Total	0.231, 0.136	100	
$D(2^3S_1)$ 2643	$D\gamma$	0.60, 0.10	0.6, 0.1	
	$D\pi$	26.1	25.6	
	$D\eta$	3.85	3.8	
	$D^*\pi$	58.8	57.6	
	$D^*\eta$	1.97	1.9	
	$D(1P_1')\pi$	0.65	0.6	
	$D_s K$	8.8	8.6	
	$D_s^* K$	1.1	1.1	
	Total	102	100	
	$D(2^1S_0)$ 2581	$D^*\pi$	79.7	99.3
$D(1^3P_0)\pi$		0.49	0.6	
Total		80	100	
$D(3^3S_1)$ 3110	$D\gamma$	0.66, 0.12	0.6, 0.1	
	$D\pi$	3.21	3.1	
	$D\rho$	0.85	0.8	
	$D\eta$	0.34	0.3	
	$D\omega$	0.25	0.2	
	$D^*\pi$	5.6	5.4	
	$D^*\rho$	3.4	3.2	
	$D^*\omega$	1.3	1.3	
	$D(2^1S_0)\pi$	8.0	7.7	
	$D(2^3S_1)\pi$	18.1	17.5	
	$D(1P_1)\pi$	18.2	17.6	
	$D(1P_1)\eta$	0.73	0.7	
	$D(1P_1')\pi$	1.1	1.0	
	$D(1P_1')\eta$	0.9	0.9	
	$D(1^3P_2)\pi$	24.3	23.5	
	$D_s^* K^*$	6.47	6.3	
	$D_s(1P_1')K$	5.1	4.9	
	Total	103	100	
	$D(3^1S_0)$ 3068	$D^*\pi$	5.2	4.9
		$D^*\rho$	9.8	9.3
$D^*\eta'$		1.2	1.2	
$D^*\omega$		3.5	3.3	
$D(2^3S_1)\pi$		26.6	25.0	
$D(1^3P_2)\pi$		45.6	43	
$D_s K^*$		2.4	2.2	
$D_s^* K$		2.4	2.3	
$D_s^* K^*$		3.4	3.2	
$D_s(1^3P_0)K$		4.0	3.8	
Total		106	100	

TABLE V: Partial widths and branching ratios for strong and electromagnetic decays for the  $4S$  charm mesons. See the caption to Table IV for further explanations.

Initial state	Final state	Width ( $cu, cd$ ) (MeV)	B.R. ( $cu, cd$ ) (%)
$D(4^3S_1)$ 3497	$D\gamma$	0.64, 0.12	0.45, 0.08
	$D(2^1S_0)\gamma$	0.43, 0.09	0.30, 0.06
	$D(3^1S_0)\gamma$	0.15, 0.03	0.11, 0.02
	$D\pi$	0.7	0.5
	$D^*\pi$	1.4	1.0
	$D(2^1S_0)\pi$	2.0	1.4
	$D(2^1S_0)\rho$	3.4	2.4
	$D(2^3S_1)\pi$	4.2	2.9
	$D(2^3S_1)\rho$	24.1	17.0
	$D(2^3S_1)\omega$	8.0	5.6
	$D(3^1S_0)\pi$	3.1	2.2
	$D(3^3S_1)\pi$	7.3	5.1
	$D(1P_1)\pi$	2.0	1.4
	$D(1P_1)\rho$	1.5	1.1
	$D(1P_1')\rho$	1.3	0.9
	$D(1^3P_2)\pi$	2.3	1.6
	$D(1^3P_2)\rho$	10.2	7.2
$D(1^3P_2)\omega$	3.6	2.5	
$D(2P_1)\pi$	13.4	9.5	
$D(2P_1')\pi$	1.3	0.9	
$D(2^3P_2)\pi$	16.1	11.4	
$D(1D_2)\pi$	9.5	6.7	
$D(1^3D_3)\pi$	10.7	7.6	
$D_s(2^3S_1)K$	1.5	1.1	
Total	142	100	
$D(4^1S_0)$ 3468	$D\rho$	0.4	0.3
	$D^*\pi$	1.4	0.9
	$D(2^1S_0)\rho$	8.7	5.6
	$D(2^1S_0)\omega$	3.0	2.0
	$D(2^3S_1)\pi$	5.4	3.5
	$D(2^3S_1)\rho$	19.1	12.4
	$D(2^3S_1)\omega$	5.7	3.7
	$D(3^3S_1)\pi$	11.0	7.1
	$D(1P_1)\rho$	4.4	2.9
	$D(1P_1)\omega$	1.6	1.0
	$D(1P_1')\rho$	1.9	1.2
	$D(1^3P_2)\pi$	2.9	1.9
	$D(1^3P_2)\rho$	10.9	7.1
	$D(1^3P_2)\omega$	3.6	2.4
	$D(2^3P_2)\pi$	33.9	22.0
$D(1^3D_3)\pi$	25.0	16.2	
$D_s(2^3S_1)K$	3.9	2.6	
$D_s(1P_1')K^*$	2.3	1.5	
$D_s(1^3P_2)K$	3.20	2.1	
Total	154	100	

TABLE VI: Partial widths and branching ratios for strong and electromagnetic decays for the  $5S$  charm mesons. See the caption of Table IV for further explanations.

Initial state	Final state	Width ( $cu, cd$ ) (MeV)	B.R. ( $cu, cd$ ) (%)	
$D(5^3S_1)$ 3837	$D\gamma$	0.61, 0.1	0.45, 0.09	
	$D(2^1S_0)\gamma$	0.56, 0.1	0.41, 0.08	
	$D(3^1S_0)\gamma$	0.32, 0.07	0.24, 0.05	
	$D(4^1S_0)\gamma$	0.10, 0.02	0.08, 0.2	
	$D^*\pi$	1.0	0.7	
	$D^*\rho$	0.7	0.5	
	$D(3^3S_1)\pi$	2.8	2.1	
	$D(4^1S_0)\pi$	1.5	1.1	
	$D(4^3S_1)\pi$	3.5	2.6	
	$D(2P_1)\pi$	2.9	2.1	
	$D(2P_1)\rho$	6.9	5.0	
	$D(2P_1)\omega$	2.4	1.7	
	$D(2^3P_2)\pi$	3.3	2.5	
	$D(2^3P_2)\rho$	19.0	14	
	$D(2^3P_2)\omega$	6.1	4.5	
	$D(3P_1)\pi$	7.4	5.4	
	$D(3P_1')\pi$	1.3	1.0	
	$D(3^3P_2)\pi$	8.9	6.5	
	$D(1D_2)\rho$	1.7	1.2	
	$D(1^3D_3)\rho$	5.8	4.32	
	$D(1^3D_3)\omega$	2.0	1.5	
	$D(2D_2)\pi$	10.7	7.9	
	$D(2^3D_3)\pi$	10.7	7.9	
	$D(1F_3)\pi$	4.4	3.2	
	$D(1^3F_4)\pi$	4.5	3.3	
	$D_s(3^3S_1)K$	2.8	2.0	
	$D_s(2^3P_2)K$	1.7	1.3	
	Total	136	100	
	$D(5^1S_0)$ 3814	$D(2^3S_1)\pi$	1.4	0.9
		$D(2^3S_1)\rho$	1.5	0.9
$D(3^3S_1)\pi$		4.2	2.7	
$D(4^3S_1)\pi$		5.3	3.4	
$D(2P_1)\rho$		13.0	8.3	
$D(2P_1)\omega$		4.2	2.7	
$D(2^3P_2)\pi$		6.0	3.9	
$D(2^3P_2)\rho$		13.8	8.8	
$D(2^3P_2)\omega$		4.2	2.7	
$D(3^3P_0)\pi$		1.1	0.7	
$D(3^3P_2)\pi$		20.1	12.9	
$D(1D_2)\rho$		3.9	2.5	
$D(1^3D_3)\pi$		1.9	1.2	
$D(1^3D_3)\rho$		5.6	3.6	
$D(1^3D_3)\omega$		1.9	1.2	
$D(2^3D_3)\pi$		28.0	18.0	
$D(1^3F_4)\pi$		12.8	8.2	
$D_s(3^3S_1)K$		5.67	3.6	
$D_s(2^3P_2)K$		5.32	3.4	
$D_s(1^3D_3)K$		2.0	1.3	
Total		156	100	

TABLE VII: Partial widths and branching ratios for strong and electromagnetic decays for the  $1P$  charm mesons. See the caption of Table IV for further explanations.

Initial state	Final state	Width ( $cu, cd$ ) (MeV)	B.R. ( $cu, cd$ ) (%)
$D(1^3P_0)$ 2399	$D^*\gamma$	0.288, 0.030	0.187, 0.019
	$D\pi$	154	99.8, 99.9
	Total	154	100
$D(1P_1)$ 2456	$D\gamma$	0.640, 0.066	6.01, 0.661
	$D^*\gamma$	0.0828, 0.0086	0.778, 0.086
	$D^*\pi$	9.92	93.2, 99.2
	Total	10.64, 10.00	100
$D(1P_1')$ 2467	$D\gamma$	0.156, 0.0161	0.097, 0.001
	$D^*\gamma$	0.386, 0.0399	0.239, 0.025
	$D^*\pi$	161	99.6, 99.9
	Total	162, 161	100
$D(1^3P_2)$ 2502	$D^*\gamma$	0.592, 0.0612	2.58, 0.27
	$D\pi$	15.3	66.6, 68.2
	$D\eta$	0.107	0.466, 0.477
	$D^*\pi$	6.98	30.4, 31.1
	Total	23.0, 22.4	100



TABLE VIII: Partial widths and branching ratios for strong decays for the  $2P$  charm mesons. See the caption for Table IV for further explanations.

Initial state	Final state	Width (MeV)	B.R. (%)
$D(2^3P_0)$ 2931	$D\pi$	25.4	13.4
	$D\eta$	1.53	0.8
	$D\eta'$	4.94	2.6
	$D^*\rho$	32.0	16.8
	$D^*\omega$	10.2	5.4
	$D(2^1S_0)\pi$	18.6	9.8
	$D(1P_1)\pi$	96.1	50.6
	$D_sK$	0.76	0.4
	Total	190	100
	$D(2P_1)$ 2924	$D\rho$	3.4
$D\omega$		1.1	0.9
$D^*\pi$		37.9	30.3
$D^*\rho$		24.4	19.5
$D^*\eta$		5.0	4.0
$D^*\omega$		8.2	6.5
$D(2^3S_1)\pi$		1.3	1.0
$D(1^3P_0)\pi$		4.9	3.9
$D(1P_1)\pi$		5.2	4.2
$D(1P_1')\pi$		2.5	2.0
$D(1^3P_2)\pi$		7.4	5.9
$D_sK^*$		14.3	11.4
$D_s^*K$		9.0	7.2
Total		125	100
$D(2P_1')$ 2961	$D\rho$	18.8	8.9
	$D\omega$	6.11	2.9
	$D^*\pi$	21.6	10.2
	$D^*\rho$	23.3	11.0
	$D^*\omega$	7.3	3.5
	$D(2^3S_1)\pi$	20.9	9.9
	$D(1P_1)\pi$	15.9	7.5
	$D(1P_1')\pi$	5.3	2.5
	$D(1^3P_2)\pi$	82.3	38.9
	$D_sK^*$	4.0	1.9
	$D_s^*K$	4.4	2.1
	Total	212	100
$D(2^3P_2)$ 2957	$D\pi$	5.0	4.4
	$D\rho$	10.6	9.3
	$D\eta$	1.3	1.2
	$D\omega$	3.5	3.0
	$D^*\pi$	17.1	15.0
	$D^*\rho$	26.3	23.0
	$D^*\eta$	2.8	2.5
	$D^*\omega$	9.2	8.1
	$D(2^1S_0)\pi$	2.40	2.1
	$D(2^3S_1)\pi$	1.4	1.2
	$D(1P_1)\pi$	5.7	5.0
	$D(1P_1')\pi$	6.5	5.7
	$D(1^3P_2)\pi$	11.9	10.4
	$D_sK$	3.7	3.2
	$D_s^*K$	5.6	4.9
	Total	114	100

TABLE IX: Partial widths and branching ratios for strong decays for the  $3^3P_0$  and  $3P_1$  charm mesons. See the caption for Table IV for further explanations.

Initial state	Final state	Width (MeV)	B.R. (%)
$D(3^3P_0)$ 3343	$D\pi$	5.57	3.40
	$D\eta$	0.478	0.292
	$D^*\rho$	0.327	0.200
	$D(2^1S_0)\pi$	11.3	6.90
	$D(3^1S_0)\pi$	5.40	3.30
	$D(1^3P_0)\rho$	2.04	1.25
	$D(1P_1)\pi$	7.90	4.82
	$D(1P_1)\rho$	6.59	4.02
	$D(1P_1)\omega$	2.21	1.35
	$D(1P_1')\rho$	8.92	5.45
	$D(1P_1')\omega$	2.94	1.80
	$D(1^3P_2)\rho$	3.51	2.14
	$D(2P_1)\pi$	44.8	27.4
	$D(2P_1')\pi$	0.289	0.176
	$D(1D_2)\pi$	43.5	26.6
	Total	163.8	100
	$D(3P_1)$ 3328	$D\rho$	1.02
$D\omega$		0.318	0.264
$D^*\pi$		4.54	3.78
$D^*\rho$		0.299	0.25
$D(2^3S_1)\pi$		15.2	12.6
$D(2^3S_1)\eta$		1.88	1.56
$D(1P_1)\rho$		17.8	14.8
$D(1P_1)\omega$		5.85	4.86
$D(1P_1')\rho$		7.71	6.41
$D(1P_1')\omega$		2.49	2.07
$D(1^3P_2)\pi$		20.5	17.0
$D(1^3P_2)\rho$		5.52	4.59
$D(1^3P_2)\eta$		2.14	1.78
$D(1^3P_2)\omega$		1.58	1.31
$D(2^3P_0)\pi$		2.54	2.11
$D(2P_1)\pi$		2.61	2.17
$D(2P_1')\pi$		1.02	0.848
$D(2^3P_2)\pi$	5.56	4.62	
$D(1D_2)\pi$	3.11	2.59	
$D(1^3D_3)\pi$	6.44	5.36	
$D_s(2^3S_1)K$	2.42	2.01	
$D_s(1^3P_2)K$	3.03	2.52	
Total	120.2	100	

TABLE X: Partial widths and branching ratios for strong decays for the  $3P_1'$  and  $3^3P_2$  charm mesons. See the caption for Table IV for further explanations.

Initial state	Final state	Width (MeV)	B.R. (%)
$D(3P_1')$ 3360	$D\rho$	1.85	0.986
	$D\omega$	0.595	0.317
	$D^*\pi$	4.54	2.42
	$D^*\rho$	0.746	0.398
	$D(2^1S_0)\rho$	3.81	2.03
	$D(2^3S_1)\pi$	11.1	5.92
	$D(3^3S_1)\pi$	6.11	3.26
	$D(1P_1)\rho$	6.73	3.59
	$D(1P_1)\omega$	2.18	1.16
	$D(1P_1')\rho$	6.00	3.20
	$D(1P_1')\omega$	2.03	1.08
	$D(1^3P_2)\pi$	7.28	3.88
	$D(1^3P_2)\rho$	11.3	6.02
	$D(1^3P_2)\omega$	3.53	1.88
	$D(2P_1)\pi$	7.70	4.10
	$D(2P_1')\pi$	2.20	1.17
	$D(2^3P_2)\pi$	35.2	18.8
	$D(1D_2)\pi$	11.0	5.86
	$D(1^3D_3)\pi$	37.9	20.2
	$D_s(2^3S_1)K$	7.40	3.94
$D_s(1^3P_2)K$	7.70	4.10	
Total	187.6	100	
$D(3^3P_2)$ 3353	$D\pi$	0.981	0.843
	$D\rho$	1.21	1.04
	$D\eta$	0.185	0.159
	$D\omega$	0.396	0.340
	$D^*\pi$	2.80	2.41
	$D(2^1S_0)\pi$	2.71	2.33
	$D(2^1S_0)\eta$	1.10	0.946
	$D(2^3S_1)\pi$	6.91	5.94
	$D(2^3S_1)\eta$	1.37	1.18
	$D(1P_1)\pi$	5.18	4.45
	$D(1P_1)\rho$	2.76	2.37
	$D(1P_1')\pi$	1.44	1.24
	$D(1P_1')\rho$	4.86	4.18
	$D(1P_1')\omega$	1.64	1.41
	$D(1^3P_2)\pi$	7.13	6.13
	$D(1^3P_2)\rho$	25.8	22.2
	$D(1^3P_2)\omega$	8.19	7.04
	$D(2P_1)\pi$	4.75	4.08
	$D(2P_1')\pi$	3.36	2.89
	$D(2^3P_2)\pi$	6.47	5.56
	$D(1D_2)\pi$	3.36	2.89
	$D(1^3D_3)\pi$	6.92	5.95
	$D_s(2^1S_0)K$	2.28	1.96
	$D_s(2^3S_1)K$	2.02	1.74
	$D_s(1P_1)K$	1.43	1.23
	$D_s(1^3P_2)K$	1.82	1.56
	Total	116.3	100

TABLE XI: Partial widths and branching ratios for strong decays for the  $4^3P_0$  and  $4P_1$  charm mesons. See the caption for Table IV for further explanations.

Initial state	Final state	Width (MeV)	B.R. (%)
$D(4^3P_0)$ 3697	$D\pi$	1.93	1.21
	$D\eta$	0.219	0.137
	$D^*\rho$	0.450	0.282
	$D(2^1S_0)\pi$	3.20	2.01
	$D(2^3S_1)\rho$	2.74	1.72
	$D(3^1S_0)\pi$	5.41	3.39
	$D(4^1S_0)\pi$	2.59	1.63
	$D(1P_1)\pi$	1.78	1.12
	$D(2P_1)\pi$	11.7	7.34
	$D(3P_1)\pi$	20.2	12.7
	$D(1D_2)\pi$	3.20	2.01
	$D(1D_2)\rho$	4.46	2.80
	$D(2D_2)\pi$	38.2	24.0
	$D(2D_2')\pi$	0.949	0.595
	$D(1F_3)\pi$	19.7	12.4
	$D_s(2^3S_1)K^*$	2.43	1.52
	$D_s(3^1S_0)K$	10.4	6.53
	$D_s(1^3P_2)K^*$	1.64	1.03
	$D_s(2P_1)K$	10.0	6.27
	$D_s(1D_2)K$	4.22	2.65
Total	159.4	100	
$D(4P_1)$ 3681	$D\rho$	0.678	0.668
	$D^*\pi$	1.08	1.06
	$D(2^3S_1)\pi$	3.61	3.56
	$D(2^3S_1)\rho$	2.60	2.56
	$D(3^3S_1)\pi$	6.96	6.86
	$D(1^3P_2)\pi$	2.75	2.71
	$D(2^3P_0)\pi$	1.10	1.08
	$D(2^3P_2)\pi$	14.4	14.2
	$D(2^3P_2)\eta$	1.86	1.83
	$D(3^3P_0)\pi$	1.30	1.28
	$D(3P_1)\pi$	1.13	1.11
	$D(3^3P_2)\pi$	3.50	3.45
	$D(1D_2)\rho$	6.58	6.49
	$D(1D_2)\omega$	1.98	1.95
	$D(1D_2')\rho$	1.16	1.14
	$D(1^3D_3)\pi$	9.16	9.03
	$D(1^3D_3)\rho$	1.73	1.71
$D(1^3D_3)\eta$	1.06	1.05	
$D(2D_2)\pi$	2.74	2.70	
$D(2^3D_3)\pi$	8.18	8.06	
$D(1F_3)\pi$	1.41	1.39	
$D(1^3F_4)\pi$	4.61	4.54	
$D_s(2^3S_1)K^*$	1.47	1.45	
$D_s(2^3P_0)K$	1.19	1.17	
$D_s(2^3P_2)K$	2.58	2.54	
$D_s(1^3D_3)K$	1.56	1.54	
Total	101.4	100	

TABLE XII: Partial widths and branching ratios for strong decays for the  $4P_1'$  and  $4^3P_2$  charm mesons. See the caption for Table IV for further explanations.

Initial state	Final state	Width (MeV)	B.R. (%)
$D(4P_1')$ 3709	$D\rho$	0.635	0.368
	$D^*\pi$	1.62	0.939
	$D(2^3S_1)\pi$	3.19	1.85
	$D(3^3S_1)\pi$	5.72	3.31
	$D(4^3S_1)\pi$	2.69	1.56
	$D(2P_1)\pi$	1.90	1.10
	$D(2^3P_2)\pi$	9.30	5.39
	$D(3P_1)\pi$	3.39	1.96
	$D(3P_1')\pi$	1.19	0.690
	$D(3^3P_2)\pi$	15.6	9.04
	$D(1D_2)\rho$	2.53	1.47
	$D(1^3D_3)\pi$	3.42	1.98
	$D(1^3D_3)\rho$	4.88	2.83
	$D(2D_2)\pi$	9.60	5.56
	$D(2^3D_3)\pi$	29.3	17.0
	$D(1F_3)\pi$	5.55	3.22
	$D(1^3F_4)\pi$	16.9	9.79
	$D_s(2^3S_1)K^*$	1.77	1.03
	$D_s(3^3S_1)K$	11.9	6.90
	$D_s(2^3P_2)K$	9.13	5.29
$D_s(1^3D_3)K$	3.82	2.21	
Total	172.6	100	
$D(4^3P_2)$ 3701	$D^*\pi$	0.698	0.757
	$D(2^3S_1)\pi$	1.88	2.04
	$D(2^3S_1)\rho$	1.99	2.16
	$D(3^1S_0)\pi$	1.18	1.28
	$D(3^3S_1)\pi$	3.15	3.42
	$D(1^3P_2)\pi$	1.29	1.40
	$D(1^3P_2)\rho$	1.30	1.41
	$D(2P_1)\pi$	3.87	4.20
	$D(2P_1)\eta$	1.17	1.27
	$D(2P_1')\pi$	1.47	1.59
	$D(2^3P_2)\pi$	5.04	5.47
	$D(3P_1)\pi$	3.13	3.40
	$D(3P_1')\pi$	1.67	1.81
	$D(3^3P_2)\pi$	3.46	3.75
	$D(1D_2)\pi$	2.58	2.80
	$D(1D_2)\rho$	1.28	1.39
	$D(1^3D_3)\pi$	2.70	2.93
	$D(1^3D_3)\rho$	9.68	10.5
	$D(1^3D_3)\omega$	2.95	3.20
	$D(2D_2)\pi$	5.12	5.55
	$D(2D_2')\pi$	0.985	1.07
	$D(2^3D_3)\pi$	6.72	7.29
	$D(1F_3)\pi$	2.14	2.32
	$D(1^3F_4)\pi$	3.58	3.88
	$D_s(2^3S_1)K^*$	1.33	1.44
	$D_s(2P_1)K$	1.76	1.91
	$D_s(2P_1')K$	1.57	1.70
	$D_s(2^3P_2)K$	1.94	2.10
Total	92.19	100	

TABLE XIII: Partial widths and branching ratios for strong and electromagnetic decays for the  $1D$  charm mesons. See the caption for Table IV for further explanations.

Initial state	Final state	Width ( $cu, cd$ ) (MeV)	B.R. ( $cu, cd$ ) (%)
$D(1^3D_1)$ 2817	$D(1^3P_0)\gamma$	0.521, 0.0538	0.223, 0.0231
	$D\pi$	53.6	23.0
	$D\rho$	19.8	8.5
	$D\eta$	10.1	4.3
	$D\omega$	6.3	2.7
	$D^*\pi$	29.3	12.5
	$D^*\eta$	4.00	1.7
	$D(1P_1)\pi$	76.4	32.7
	$D(1P_1')\pi$	2.1	0.9
	$D(1^3P_2)\pi$	0.6	0.3
	$D_sK$	22.8	9.8
$D_s^*K$	7.4	3.2	
Total	234	100	
$D(1D_2)$ 2816	$D(1P_1)\gamma$	0.642, 0.066	0.61, 0.064
	$D\rho$	61.2	58.2
	$D\omega$	19.6	18.7
	$D^*\pi$	21.2	20.2
	Total	105	100
$D(1D_2')$ 2845	$D\rho$	5.85	2.4
	$D^*\pi$	93.3	38.3
	$D^*\rho$	5.0	2.1
	$D^*\eta$	14.7	6.0
	$D(1^3P_2)\pi$	89.9	36.9
	$D_s^*K$	29.5	12.1
Total	244	100	
$D(1^3D_3)$ 2833	$D(1^3P_2)\gamma$	0.69, 0.07	1.34, 0.14
	$D\pi$	20.1	39.2
	$D\rho$	1.30	2.5
	$D\eta$	1.24	2.4
	$D^*\pi$	15.5	30.2
	$D^*\rho$	7.56	14.8
	$D^*\omega$	1.1	2.2
	$D(1^3P_2)\pi$	0.9	1.8
	$D_sK$	1.1	2.20
	Total	51	100

TABLE XIV: Partial widths and branching ratios for strong decays for the  $2^3D_1$  and  $2D_2$  charm mesons. See the caption for Table IV for further explanations.

Initial state	Final state	Width (MeV)	B.R. (%)	
$D(2^3D_1)$ 3231	$D\pi$	11.0	5.14	
	$D\rho$	1.33	0.621	
	$D\eta$	1.23	0.575	
	$D\omega$	0.418	0.195	
	$D^*\pi$	4.41	2.06	
	$D^*\rho$	29.7	13.9	
	$D^*\omega$	9.73	4.54	
	$D(2^1S_0)\pi$	6.07	2.84	
	$D(2^1S_0)\eta$	2.53	1.18	
	$D(2^3S_1)\pi$	4.37	2.04	
	$D(1P_1)\pi$	25.3	11.8	
	$D(1^3P_2)\pi$	14.8	6.91	
	$D(2P_1)\pi$	18.3	8.55	
	$D(1D_2)\pi$	53.7	25.1	
	$D_s^*K^*$	3.14	1.47	
	$D_s(2^1S_0)K$	4.17	1.95	
	$D_s(1P_1)K$	12.0	5.61	
	Total	214.1	100	
	$D(2D_2)$ 3212	$D\rho$	5.37	6.33
		$D\omega$	1.71	2.02
$D^*\pi$		8.08	9.53	
$D^*\rho$		12.5	14.7	
$D^*\eta$		1.87	2.2	
$D^*\omega$		4.09	4.82	
$D(2^3S_1)\pi$		10.1	11.9	
$D(1^3P_0)\pi$		3.18	3.75	
$D(1P_1)\pi$		3.35	3.95	
$D(1P_1)\eta$		0.384	0.453	
$D(1P_1')\pi$		3.18	3.75	
$D(1^3P_2)\pi$		14.0	16.5	
$D(1D_2)\pi$		2.81	3.31	
$D_s^*K$		3.91	4.61	
$D_s^*K^*$		2.88	3.40	
$D_s(1^3P_0)K$		1.03	1.21	
Total		84.8	100	

TABLE XV: Partial widths and branching ratios for strong decays for the  $2D_2'$  and  $2^3D_3$  charm mesons. See the caption for Table IV for further explanations.

Initial state	Final state	Width (MeV)	B.R. (%)
$D(2D_2')$ 3248	$D\rho$	5.89	2.71
	$D\omega$	1.97	0.907
	$D^*\pi$	17.0	7.83
	$D^*\rho$	15.9	7.32
	$D^*\eta$	1.38	0.636
	$D^*\eta'$	0.479	0.221
	$D^*\omega$	5.21	2.40
	$D(2^3S_1)\pi$	12.2	5.62
	$D(2^3S_1)\eta$	2.42	1.11
	$D(1P_1)\pi$	4.66	2.15
	$D(1P_1)\rho$	2.74	1.26
	$D(1P_1')\pi$	3.62	1.67
	$D(1^3P_2)\pi$	32.2	14.8
	$D(1^3P_2)\eta$	2.38	1.10
	$D(2^3P_2)\pi$	19.7	9.07
	$D(1D_2)\pi$	4.78	2.20
	$D(1^3D_3)\pi$	56.1	25.8
$D_s^*K^*$	3.00	1.38	
$D_s(1^3P_2)K$	15.1	6.96	
Total	217.1	100	
$D(2^3D_3)$ 3226	$D\rho$	1.96	2.69
	$D\eta$	0.108	0.148
	$D\eta'$	0.261	0.359
	$D^*\pi$	2.16	2.97
	$D^*\rho$	8.28	11.4
	$D^*\eta$	0.708	0.973
	$D^*\eta'$	0.321	0.441
	$D^*\omega$	2.63	3.62
	$D(2^1S_0)\pi$	7.24	9.95
	$D(2^3S_1)\pi$	6.82	9.38
	$D(1P_1)\pi$	8.68	11.9
	$D(1P_1')\pi$	5.20	7.15
	$D(1^3P_2)\pi$	10.7	14.7
	$D(1D_2')\pi$	1.12	1.54
	$D(1^3D_3)\pi$	3.53	4.85
	$D_s^*K$	1.71	2.35
	$D_s^*K^*$	3.74	5.14
$D_s(1P_1')K$	1.30	1.79	
$D_s(1^3P_2)K$	0.900	1.24	
Total	72.7	100	

TABLE XVI: Partial widths and branching ratios for strong decays for the  $3^3D_1$  and  $3D_2$  charm mesons. See the caption for Table IV for further explanations.

Initial state	Final state	Width (MeV)	B.R. (%)
$D(3^3D_1)$ 3588	$D\pi$	2.99	1.47
	$D^*\pi$	1.12	0.551
	$D^*\rho$	2.33	1.15
	$D(2^1S_0)\pi$	3.77	1.86
	$D(2^3S_1)\pi$	2.21	1.09
	$D(2^3S_1)\rho$	15.1	7.43
	$D(2^3S_1)\omega$	4.74	2.33
	$D(1P_1)\pi$	4.24	2.09
	$D(1^3P_2)\rho$	13.3	6.55
	$D(1^3P_2)\omega$	4.26	2.10
	$D(2P_1)\pi$	14.7	7.24
	$D(2^3P_2)\pi$	5.76	2.84
	$D(3P_1)\pi$	6.60	3.25
	$D(1D_2)\pi$	8.49	4.18
	$D(1^3D_3)\pi$	6.25	3.08
	$D(2D_2)\pi$	31.7	15.6
	$D(1F_3)\pi$	26.5	13.0
	$D_s(2P_1)K$	13.9	6.84
	$D_s(1D_2)K$	9.09	4.48
	Total	203.1	100
$D(3D_2)$ 3566	$D\rho$	2.01	2.11
	$D\omega$	0.653	0.684
	$D^*\pi$	1.74	1.82
	$D^*\rho$	1.49	1.56
	$D(2^1S_0)\rho$	0.970	1.02
	$D(2^3S_1)\pi$	2.93	3.07
	$D(2^3S_1)\rho$	8.69	9.11
	$D(2^3S_1)\eta$	1.55	1.62
	$D(2^3S_1)\omega$	2.86	3.00
	$D(3^3S_1)\pi$	4.79	5.02
	$D(1P_1)\rho$	1.79	1.88
	$D(1^3P_2)\pi$	4.38	4.59
	$D(1^3P_2)\rho$	6.20	6.50
	$D(1^3P_2)\eta$	1.09	1.14
	$D(1^3P_2)\omega$	2.03	2.13
	$D(2^3P_0)\pi$	1.73	1.81
	$D(2P_1)\pi$	1.76	1.84
	$D(2P'_1)\pi$	1.49	1.56
	$D(2^3P_2)\pi$	13.5	14.1
	$D(1D_2)\pi$	2.03	2.13
	$D(1^3D_3)\pi$	8.65	9.06
	$D(2D_2)\pi$	1.97	2.06
	$D(1F_3)\pi$	1.75	1.83
	$D_s(2^3S_1)K$	3.86	4.04
	$D_s(1^3P_2)K$	1.88	1.97
	Total	95.4	100

TABLE XVII: Partial widths and branching ratios for strong decays for the  $3D'_2$  and  $3^3D_3$  charm mesons. See the caption for Table IV for further explanations.

Initial state	Final state	Width (MeV)	B.R. (%)
$D(3D'_2)$ 3600	$D^*\pi$	4.53	2.14
	$D^*\rho$	2.09	0.989
	$D(2^1S_0)\rho$	7.28	3.44
	$D(2^1S_0)\omega$	2.37	1.12
	$D(2^3S_1)\pi$	6.22	2.94
	$D(2^3S_1)\rho$	10.2	4.82
	$D(2^3S_1)\omega$	3.32	1.57
	$D(3^3S_1)\pi$	3.14	1.49
	$D(1P_1)\rho$	4.34	2.05
	$D(1^3P_2)\pi$	5.84	2.76
	$D(1^3P_2)\rho$	6.54	3.09
	$D(1^3P_2)\omega$	2.19	1.04
	$D(2^3P_2)\pi$	16.6	7.85
	$D(3^3P_2)\pi$	7.16	3.39
	$D(1D_2)\pi$	3.13	1.48
	$D(1^3D_3)\pi$	11.5	5.44
	$D(2D_2)\pi$	3.44	1.63
$D(2^3D_3)\pi$	30.4	14.4	
$D(1F_3)\pi$	3.32	1.57	
$D(1^3F_4)\pi$	27.6	13.1	
$D_s(2^3P_2)K$	16.3	7.71	
$D_s(1^3D_3)K$	9.18	4.34	
Total	211.4	100	
$D(3^3D_3)$ 3579	$D^*\pi$	0.645	0.716
	$D^*\rho$	2.62	2.91
	$D^*\omega$	0.835	0.926
	$D(2^1S_0)\rho$	3.32	3.68
	$D(2^1S_0)\omega$	1.07	1.19
	$D(2^3S_1)\pi$	0.798	0.885
	$D(2^3S_1)\rho$	8.09	8.98
	$D(2^3S_1)\omega$	2.87	3.18
	$D(3^1S_0)\pi$	3.42	3.79
	$D(3^3S_1)\pi$	3.27	3.63
	$D(1P_1)\rho$	1.74	1.93
	$D(1P'_1)\pi$	1.36	1.51
	$D(1^3P_2)\pi$	1.76	1.95
	$D(1^3P_2)\rho$	5.21	5.78
	$D(1^3P_2)\omega$	1.81	2.01
	$D(2P_1)\pi$	9.40	10.4
	$D(2P'_1)\pi$	2.74	3.04
$D(2^3P_2)\pi$	7.50	8.32	
$D(1D_2)\pi$	4.40	4.88	
$D(1^3D_3)\pi$	4.92	5.46	
$D(2^3D_3)\pi$	2.42	2.68	
$D(1^3F_4)\pi$	2.36	2.62	
$D_s(2^1S_0)K$	1.36	1.51	
$D_s(2^3S_1)K$	1.96	2.17	
$D_s(1^3P_2)K^*$	1.23	1.36	
$D_s(1D'_2)K$	0.960	1.07	
Total	90.13	100	

TABLE XVIII: Partial widths and branching ratios for strong and electromagnetic decays for the  $1F$  charm mesons. See the caption for Table IV for further explanations.

Initial state	Final state	Width ( $cu, cd$ ) (MeV)	B.R. ( $cu, cd$ ) (%)
$D(1^3F_2)$ 3132	$D(1^3D_1)\gamma$	0.70, 0.073	0.29, 0.03
	$D\pi$	23.1	9.5
	$D\rho$	16.4	6.7
	$D\eta$	4.4	1.8
	$D\omega$	5.4	2.2
	$D^*\pi$	18.5	7.6
	$D^*\rho$	16.0	6.6
	$D^*\eta$	3.15	1.3
	$D^*\omega$	5.1	2.1
	$D(1P_1)\pi$	52.9	21.7
	$D(1P_1)\eta$	6.60	2.7
	$D(1^3P_2)\pi$	10.3	4.2
	$D(1D_2)\pi$	43.8	18.0
	$D_sK$	7.92	3.2
	$D_s^*K$	5.11	2.1
	$D_s(1P_1)K$	9.5	3.9
	Total	243	100
$D(1F_3)$ 3108	$D(1D_2)\gamma$	0.73, 0.075	0.58, 0.060
	$D\rho$	38.9	31
	$D\omega$	12.9	10.2
	$D^*\pi$	25.1	20.0
	$D^*\rho$	25.6	20.3
	$D^*\omega$	8.27	6.6
	$D(1^3P_2)\pi$	1.93	1.5
	$D_sK^*$	4.10	3.3
	Total	126	100
$D(1F_3')$ 3143	$D(1D_2)\gamma$	0.74, 0.077	0.28, 0.0296
	$D\rho$	9.8	3.6
	$D\omega$	3.1	1.2
	$D^*\pi$	46.2	17.2
	$D^*\rho$	29.5	11.0
	$D^*\eta$	8.2	3.1
	$D^*\omega$	9.6	3.6
	$D(2^3S_1)\pi$	5.1	1.9
	$D(1^3P_2)\pi$	69.7	25.9
	$D(1^3P_2)\eta$	6.8	2.5
	$D(1^3D_3)\pi$	50.3	18.7
	$D_s^*K$	13.9	5.2
	$D_s(1^3P_2)K$	7.5	2.8
	Total	269	100
	$D(1^3F_4)$ 3113	$D(1^3D_3)\gamma$	0.75, 0.077
$D\pi$		15.8	12.2
$D\rho$		4.0	3.1
$D\eta$		1.4	1.1
$D^*\pi$		15.2	11.8
$D^*\rho$		59.1	45.7
$D^*\omega$		19.2	14.8
$D(1P_1)\pi$		1.7	1.4
$D(1^3P_2)\pi$		4.1	3.2
Total		129	100

TABLE XIX: Partial widths and branching ratios for strong decays for the  $2^3F_2$  and  $2F_3$  charm mesons. See the caption for Table IV for further explanations.

Initial state	Final state	Width (MeV)	B.R. (%)
$D(2^3F_2)$ 3490	$D\pi$	6.34	2.84
	$D\rho$	2.35	1.05
	$D^*\pi$	4.13	1.85
	$D^*\rho$	9.98	4.47
	$D^*\omega$	3.32	1.49
	$D(2^1S_0)\rho$	4.60	2.06
	$D(1^3P_0)\rho$	2.69	1.20
	$D(1P_1)\pi$	12.6	5.64
	$D(1P_1)\rho$	6.13	2.74
	$D(1P_1')\rho$	4.70	2.10
	$D(1^3P_2)\pi$	5.89	2.64
	$D(1^3P_2)\rho$	4.95	2.22
	$D(2P_1)\pi$	11.4	5.10
	$D(2^3P_2)\pi$	4.76	2.13
	$D(1D_2)\pi$	24.5	11.0
	$D(1D_2)\eta$	2.40	1.07
	$D(1^3D_3)\pi$	7.33	3.28
	$D(2D_2)\pi$	15.1	6.76
	$D(1F_3)\pi$	32.5	14.5
	$D_s(2^1S_0)K$	4.38	1.96
	$D_s(2^3S_1)K$	2.72	1.22
$D_s(1D_2)K$	14.9	6.67	
Total	223	100	
$D(2F_3)$ 3461	$D\rho$	6.37	5.96
	$D\omega$	2.08	1.95
	$D^*\rho$	5.51	5.16
	$D^*\omega$	1.81	1.69
	$D(2^1S_0)\rho$	7.67	7.18
	$D(2^1S_0)\omega$	2.30	2.15
	$D(2^3S_1)\pi$	15.4	14.4
	$D(2^3S_1)\rho$	1.16	1.09
	$D(1P_1)\rho$	7.23	6.77
	$D(1P_1)\omega$	2.50	2.34
	$D(1P_1')\pi$	1.38	1.29
	$D(1P_1')\rho$	3.40	3.18
	$D(1P_1')\omega$	1.07	1.00
	$D(1^3P_2)\pi$	14.2	13.3
	$D(1^3P_2)\rho$	5.55	5.20
	$D(1^3P_2)\omega$	1.81	1.69
	$D(2^3P_0)\pi$	1.08	1.01
	$D(2P_1)\pi$	1.99	1.86
	$D(2^3P_2)\pi$	1.61	1.51
$D(1^3D_1)\pi$	1.71	1.60	
$D(1D_2)\pi$	3.33	3.12	
$D(1^3D_3)\pi$	2.36	2.21	
Total	106.8	100	

TABLE XX: Partial widths and branching ratios for strong decays for the  $2F_3'$  and  $2^3F_4$  charm mesons. See the caption for Table IV for further explanations.

Initial state	Final state	Width (MeV)	B.R. (%)
$D(2F_3')$ 3498	$D^*\pi$	11.9	5.27
	$D^*\rho$	6.21	2.75
	$D(2^3S_1)\pi$	3.40	1.51
	$D(2^3S_1)\rho$	3.90	1.73
	$D(2^3S_1)\eta$	2.54	1.13
	$D(3^3S_1)\pi$	2.36	1.05
	$D(1P_1)\rho$	3.20	1.42
	$D(1P_1')\pi$	1.43	0.634
	$D(1P_1')\rho$	4.76	2.11
	$D(1^3P_2)\pi$	17.4	7.71
	$D(1^3P_2)\rho$	11.1	4.92
	$D(1^3P_2)\omega$	3.66	1.62
	$D(2P_1)\pi$	2.87	1.27
	$D(2^3P_2)\pi$	15.1	6.69
	$D(1D_2)\pi$	4.38	1.94
	$D(1^3D_3)\pi$	29.5	13.1
	$D(1^3D_3)\eta$	2.81	1.24
	$D(2^3D_3)\pi$	15.8	7.00
	$D(1^3F_4)\pi$	34.9	15.5
	$D_s(2^3S_1)K$	6.83	3.03
	$D_s(1^3P_2)K$	2.54	1.13
	$D_s(1^3D_3)K$	16.2	7.18
	Total		225.7
$D(2^3F_4)$ 3466	$D\pi$	0.829	0.849
	$D^*\rho$	8.98	9.20
	$D^*\eta'$	0.165	0.169
	$D^*\omega$	2.90	2.97
	$D(2^1S_0)\pi$	7.50	7.68
	$D(2^3S_1)\pi$	8.47	8.67
	$D(2^3S_1)\rho$	3.42	3.50
	$D(1^3P_0)\rho$	1.49	1.53
	$D(1P_1)\pi$	6.42	6.57
	$D(1P_1)\rho$	1.90	1.95
	$D(1P_1')\pi$	2.01	2.06
	$D(1P_1')\rho$	2.96	3.03
	$D(1^3P_2)\pi$	5.97	6.11
	$D(1^3P_2)\rho$	13.8	14.1
	$D(1^3P_2)\omega$	4.81	4.93
	$D(2P_1)\pi$	1.44	1.47
	$D(2P_1')\pi$	1.50	1.54
	$D(2^3P_2)\pi$	2.94	3.01
	$D(1D_2)\pi$	1.30	1.33
	$D(1D_2')\pi$	2.30	2.36
	$D(1^3D_3)\pi$	4.67	4.78
	$D(1^3F_4)\pi$	1.27	1.30
	$D_s(1P_1')K$	1.10	1.13
$D_s(1^3P_2)K$	1.10	1.13	
Total		97.6	100

TABLE XXI: Partial widths and branching ratios for strong and electromagnetic decays for the  $1^3G_3$  and  $1G_4$  charm mesons. See the caption for Table IV for further explanations.

Initial state	Final state	Width ( $cu, cd$ ) (MeV)	B.R. ( $cu, cd$ ) (%)
$D(1^3G_3)$ 3397	$D(1^3F_2)\gamma$	0.74, 0.076	0.32, 0.033
	$D\pi$	10.2	4.4
	$D\rho$	8.48	3.6
	$D\eta$	1.90	0.81
	$D\eta'$	1.6	0.7
	$D\omega$	2.82	1.2
	$D^*\pi$	9.7	4.1
	$D^*\rho$	19.4	8.3
	$D^*\omega$	6.3	2.7
	$D(2^1S_0)\pi$	5.6	2.4
	$D(2^3S_1)\pi$	3.5	1.5
	$D(1P_1)\pi$	30.7	13.1
	$D(1P_1)\rho$	11.9	5.1
	$D(1P_1)\eta$	5.6	2.4
	$D(1P_1)\omega$	3.7	1.6
	$D(1^3P_2)\pi$	11.3	4.8
	$D(2P_1)\pi$	5.4	2.3
	$D(1D_2)\pi$	36.6	15.6
	$D(1^3D_3)\pi$	3.6	1.6
	$D(1F_3)\pi$	24.6	10.5
	$D_sK$	2.6	1.1
	$D_s(1P_1)K$	9.3	4.0
	Total		234
$D(1G_4)$ 3364	$D(1F_3)\gamma$	0.76, 0.079	0.62, 0.064
	$D\rho$	18.5	15.0
	$D\omega$	6.2	5.0
	$D^*\pi$	20.3	16.5
	$D^*\rho$	21.0	17.0
	$D^*\eta$	1.8	1.5
	$D^*\omega$	6.9	5.6
	$D(2^3S_1)\pi$	1.5	1.2
	$D(1^3P_0)\pi$	2.1	1.7
	$D(1P_1)\pi$	2.9	2.3
	$D(1P_1)\rho$	18.8	15.2
	$D(1P_1)\omega$	5.7	4.6
	$D(1P_1')\pi$	2.0	1.7
$D(1^3P_2)\pi$	4.2	3.4	
$D(1^3P_2)\rho$	2.2	1.8	
$D_sK^*$	2.1	1.7	
$D_s^*K^*$	1.3	1.1	
Total		123	100

TABLE XXII: Partial widths and branching ratios for strong and electromagnetic decays for the  $1G'_4$  and  $1^3G_5$  charm mesons. See the caption for Table IV for further explanations.

Initial state	Final state	Width ( $cu, cd$ ) (MeV)	B.R. ( $cu, cd$ ) (%)	
$D(1G'_4)$ 3399	$D(1F'_3)\gamma$	0.75, 0.078	0.30, 0.031	
	$D\rho$	9.0	3.5	
	$D\omega$	2.9	1.2	
	$D^*\pi$	22.0	8.6	
	$D^*\rho$	23.6	9.3	
	$D^*\eta$	4.0	1.6	
	$D^*\eta'$	2.45	1.0	
	$D^*\omega$	7.8	3.0	
	$D(2^3S_1)\pi$	9.2	3.6	
	$D(1P_1)\pi$	3.4	1.4	
	$D(1^3P_2)\pi$	43.2	17.0	
	$D(1^3P_2)\rho$	11.1	4.4	
	$D(1^3P_2)\eta$	7.6	3.0	
	$D(1^3P_2)\omega$	3.3	1.3	
	$D(2^3P_2)\pi$	5.6	2.2	
	$D(1^3D_3)\pi$	43.9	17.2	
	$D(1^3F_4)\pi$	28.2	11.1	
	$D_s^*K$	5.4	2.1	
	$D_s(1^3P_2)K$	11.9	4.7	
	Total		254	100
$D(1^3G_5)$ 3362	$D(1^3F_4)\gamma$	0.78, 0.080	0.66, 0.068	
	$D\pi$	10.0	8.4	
	$D\rho$	3.9	3.3	
	$D\eta$	1.0	0.9	
	$D\omega$	1.2	1.1	
	$D^*\pi$	11.2	9.5	
	$D^*\rho$	38.3	32.4	
	$D^*\omega$	12.6	10.6	
	$D(2^1S_0)\pi$	1.3	1.1	
	$D(1P_1)\pi$	3.0	2.6	
	$D(1P'_1)\pi$	2.8	2.3	
	$D(1^3P_2)\pi$	6.2	5.2	
	$D(1^3P_2)\rho$	13.1	11.1	
	$D(1^3P_2)\omega$	3.7	3.1	
	$D(1^3D_3)\pi$ 5	1.5	1.2	
	$D_s^*K^*$	2.9	2.4	
	Total		118	100

TABLE XXIII: Partial widths and branching ratios for strong decays for the  $2^3G_3$  and  $2G_4$  charm mesons. See the caption for Table IV for further explanations.

Initial state	Final state	Width (MeV)	B.R. (%)
$D(2^3G_3)$ 3721	$D\pi$	3.66	1.61
	$D\rho$	2.03	0.895
	$D^*\pi$	2.98	1.31
	$D^*\rho$	2.14	0.943
	$D(2^1S_0)\rho$	3.40	1.50
	$D(2^3S_1)\rho$	8.66	3.82
	$D(3^1S_0)\pi$	2.87	1.26
	$D(1P_1)\pi$	7.46	3.29
	$D(1P_1)\rho$	2.99	1.32
	$D(1P'_1)\rho$	3.33	1.47
	$D(1^3P_2)\rho$	7.79	3.43
	$D(2P_1)\pi$	5.00	2.20
	$D(2^3P_2)\pi$	5.63	2.48
	$D(3P_1)\pi$	3.29	1.45
	$D(1D_2)\pi$	12.7	5.60
	$D(1D_2)\rho$	9.12	4.02
	$D(1^3D_3)\pi$	5.64	2.49
	$D(2D_2)\pi$	11.9	5.24
	$D(1F_3)\pi$	19.0	8.37
	$D(1^3F_4)\pi$	3.04	1.34
$D(2F_3)\pi$	11.2	4.94	
$D(1G_4)\pi$	19.7	8.68	
$D_s(2P_1)K$	6.52	2.87	
$D_s(1F_3)K$	12.9	5.69	
Total		226.9	100
$D(2G_4)$ 3686	$D\rho$	4.85	3.72
	$D\omega$	1.60	1.23
	$D^*\rho$	3.16	2.42
	$D^*\omega$	1.04	0.797
	$D(2^1S_0)\rho$	7.33	5.62
	$D(2^1S_0)\omega$	2.45	1.88
	$D(2^3S_1)\pi$	12.4	9.50
	$D(2^3S_1)\rho$	8.01	6.14
	$D(2^3S_1)\omega$	2.58	1.98
	$D(1P_1)\rho$	3.32	2.54
	$D(1P'_1)\rho$	2.72	2.08
	$D(1^3P_2)\pi$	9.39	7.19
	$D(1^3P_2)\rho$	4.96	3.80
	$D(1^3P_2)\omega$	1.60	1.23
	$D(2^3P_0)\pi$	1.99	1.52
	$D(2P_1)\pi$	2.70	2.07
	$D(2^3P_2)\pi$	4.61	3.53
	$D(1D_2)\pi$	2.22	1.70
	$D(1D_2)\rho$	17.4	13.3
	$D(1D_2)\omega$	5.81	4.45
$D(1^3D_3)\pi$	3.71	2.84	
$D(1^3D_3)\rho$	2.27	1.74	
$D(1F_3)\pi$	1.64	1.26	
Total		130.5	100



TABLE XXIV: Partial widths and branching ratios for strong decays for the  $2G'_4$  and  $2^3G_5$  charm mesons. See the caption for Table IV for further explanations.

Initial state	Final state	Width (MeV)	B.R. (%)	
$D(2G'_4)$ 3722	$D^*\pi$	7.51	3.16	
	$D^*\rho$	3.49	1.47	
	$D(2^1S_0)\rho$	4.08	1.72	
	$D(2^3S_1)\rho$	9.51	4.00	
	$D(3^3S_1)\pi$	5.08	2.14	
	$D(1P_1)\rho$	3.52	1.48	
	$D(1P'_1)\rho$	3.06	1.29	
	$D(1^3P_2)\pi$	10.8	4.55	
	$D(1^3P_2)\rho$	7.31	3.08	
	$D(2P_1)\pi$	3.04	1.28	
	$D(2^3P_2)\pi$	7.56	3.18	
	$D(2^3P_2)\eta$	3.40	1.43	
	$D(3^3P_2)\pi$	3.43	1.44	
	$D(1^3D_3)\pi$	16.3	6.86	
	$D(1^3D_3)\rho$	11.6	4.88	
	$D(1^3D_3)\omega$	3.91	1.65	
	$D(2^3D_3)\pi$	13.5	5.68	
	$D(1^3F_4)\pi$	21.8	9.18	
	$D(2^3F_4)\pi$	11.7	4.93	
	$D(1^3G_5)\pi$	21.3	8.97	
	$D_s(2^3P_2)K$	6.93	2.92	
	$D_s(1^3D_3)K$	3.75	1.58	
	$D_s(1^3F_4)K$	13.7	5.77	
	Total		237.6	100
	$D(2^3G_5)$ 3685	$D\pi$	1.63	1.27
		$D^*\pi$	0.685	0.532
		$D^*\rho$	8.08	6.27
		$D^*\omega$	2.64	2.05
		$D(2^1S_0)\pi$	4.71	3.66
		$D(2^1S_0)\rho$	1.40	1.09
$D(2^3S_1)\pi$		6.14	4.77	
$D(2^3S_1)\rho$		13.9	10.8	
$D(2^3S_1)\omega$		4.54	3.52	
$D(1P_1)\pi$		3.26	2.53	
$D(1P_1)\rho$		1.64	1.27	
$D(1P'_1)\rho$		2.09	1.62	
$D(1^3P_2)\pi$		2.68	2.08	
$D(1^3P_2)\rho$		5.23	4.06	
$D(2P_1)\pi$		3.36	2.61	
$D(2P'_1)\pi$		2.99	2.32	
$D(2^3P_2)\pi$		5.08	3.94	
$D(1D_2)\pi$		1.88	1.46	
$D(1D'_2)\pi$		1.78	1.38	
$D(1^3D_3)\pi$		3.76	2.92	
$D(1^3D_3)\rho$		22.2	17.2	
$D(1^3D_3)\omega$		7.22	5.60	
$D(1^3F_4)\pi$		2.07	1.61	
$D_s(1^3P_2)K^*$		2.34	1.82	
Total			128.8	100

TABLE XXV: Partial widths and branching ratios for electromagnetic and strong decays for the  $1S$ ,  $2S$  and  $3S$  charm-strange mesons. See the caption for Table IV for further explanations.

Initial state	Final state	Width (MeV)	B.R. (%)
$D_s^*$ 2129	$D_s\gamma$	0.00103	100
	No Strong Decays		
	Total	0.00103	100
$D_s(2^3S_1)$ 2732	$DK$	40.1	32.5
	$D^*K$	72.3	58.6
	$D_s\eta$	7.35	5.96
	$D_s^*\eta$	3.65	2.96
	Total	123.4	100
$D_s(2^1S_0)$ 2673	$D^*K$	73.6	100
	Total	73.6	100
$D_s(3^3S_1)$ 3193	$DK$	7.71	6.28
	$DK^*$	3.52	2.87
	$D^*K$	12.8	10.4
	$D^*K^*$	4.89	3.98
	$D(2^1S_0)K$	13.8	11.2
	$D(2^3S_1)K$	14.3	11.6
	$D(1P_1)K$	24.8	20.2
	$D(1P'_1)K$	0.642	0.523
	$D(1^3P_2)K$	26.3	21.4
	$D_s\eta$	0.269	0.219
	$D_s\eta'$	0.245	0.199
	$D_s\phi$	1.59	1.29
	$D_s^*\eta'$	1.85	1.51
	$D_s^*\phi$	6.51	5.30
	$D_s(1P_1)\eta$	0.949	0.773
$D_s(1P'_1)\eta$	2.39	1.95	
$D_s(1^3P_2)\eta$	0.337	0.274	
	Total	122.8	100
$D_s(3^1S_0)$ 3154	$DK^*$	1.21	1.53
	$D^*K$	11.9	15.0
	$D^*K^*$	17.2	21.7
	$D(2^3S_1)K$	3.81	4.81
	$D(1^3P_2)K$	36.5	46.1
	$D_s\phi$	3.85	4.86
	$D_s^*\eta$	0.335	0.423
	$D_s^*\eta'$	2.37	2.99
	$D_s^*\phi$	0.357	0.451
	$D_s(1^3P_0)\eta$	1.63	2.06
	Total	79.2	100

TABLE XXVI: Partial widths and branching ratios for strong decays for the  $4^3S_1$  and  $4^1S_0$  charm-strange mesons. See the caption for Table IV for further explanations.

Initial state	Final state	Width (MeV)	B.R. (%)
$D_s(4^3S_1)$ 3575	$DK$	2.63	1.53
	$DK^*$	3.2	1.87
	$D^*K$	5.71	3.33
	$D^*K^*$	2.27	1.32
	$D(2^1S_0)K$	4.06	2.37
	$D(2^1S_0)K^*$	8.47	4.94
	$D(2^3S_1)K$	6.45	3.76
	$D(2^3S_1)K^*$	32.4	18.9
	$D(1P_1)K$	4.47	2.61
	$D(1P_1)K^*$	3.14	1.83
	$D(1P_1')K^*$	2.92	1.70
	$D(1^3P_2)K$	4.4	2.57
	$D(1^3P_2)K^*$	20.5	12.0
	$D(2P_1)K$	20.2	11.8
	$D(2^3P_2)K$	17.1	9.97
	$D(1D_2)K$	12.8	7.46
	$D(1^3D_3)K$	12.8	7.46
	$D_s^*\phi$	0.502	0.293
	Total	171.5	100
	$D_s(4^1S_0)$ 3547	$DK^*$	3.16
$D^*K$		6.48	4.87
$D(2^1S_0)K^*$		17.5	13.2
$D(2^3S_1)K$		6.32	4.75
$D(2^3S_1)K^*$		6.5	4.88
$D(1P_1)K^*$		9.47	7.12
$D(1P_1')K^*$		3.85	2.89
$D(1^3P_2)K$		4.68	3.52
$D(1^3P_2)K^*$		20.9	15.7
$D(2^3P_2)K$		22.6	17.0
$D(1^3D_3)K$		24.4	18.3
Total	133.1	100	

TABLE XXVII: Partial widths and branching ratios for strong decays for the  $5^3S_1$  and  $5^1S_0$  charm-strange mesons. See the caption for Table IV for further explanations.

Initial state	Final state	Width (MeV)	B.R. (%)	
$D_s(5^3S_1)$ 3912	$DK$	1.10	0.642	
	$DK^*$	1.95	1.14	
	$D^*K$	2.94	1.72	
	$D^*K^*$	3.73	2.18	
	$D(2^1S_0)K$	1.60	0.933	
	$D(2^3S_1)K$	3.19	1.86	
	$D(3^1S_0)K$	2.31	1.35	
	$D(3^3S_1)K$	3.08	1.80	
	$D(1P_1)K$	1.85	1.08	
	$D(1^3P_2)K$	2.13	1.24	
	$D(2P_1)K$	5.44	3.17	
	$D(2P_1)K^*$	13.6	7.93	
	$D(2^3P_2)K$	5.03	2.93	
	$D(2^3P_2)K^*$	24.6	14.4	
	$D(3P_1)K$	10.6	6.18	
	$D(3P_1')K$	3.07	1.79	
	$D(3^3P_2)K$	6.67	3.89	
	$D(1D_2)K$	2.30	1.34	
	$D(1D_2)K^*$	3.97	2.32	
	$D(1^3D_3)K$	2.16	1.26	
	$D(1^3D_3)K^*$	12.4	7.23	
	$D(2D_2)K$	17.5	10.2	
	$D(2^3D_3)K$	15.0	8.75	
	$D(1F_3)K$	6.82	3.98	
	$D(1^3F_4)K$	6.60	3.85	
	Total		171.4	100
	$D_s(5^1S_0)$ 3894	$DK^*$	2.06	1.23
$D^*K$		3.34	1.99	
$D(2^3S_1)K$		3.62	2.16	
$D(2^3S_1)K^*$		4.13	2.47	
$D(3^3S_1)K$		2.42	1.45	
$D(1^3P_2)K$		2.35	1.40	
$D(1^3P_2)K^*$		2.05	1.22	
$D(2P_1)K^*$		21.9	13.1	
$D(2P_1')K^*$		10.0	5.97	
$D(2^3P_2)K$		6.28	3.75	
$D(2^3P_2)K^*$		12.2	7.29	
$D(3^3P_0)K$		2.90	1.73	
$D(3^3P_2)K$		6.45	3.85	
$D(1D_2)K^*$		9.88	5.90	
$D(1^3D_3)K$		2.45	1.46	
$D(1^3D_3)K^*$		12.4	7.41	
$D(2^3D_3)K$		30.7	18.3	
$D(1^3F_4)K$		16.9	10.1	
Total		167.4	100	

TABLE XXVIII: Partial widths and branching ratios for strong and electromagnetic decays for the  $1P$  charm-strange mesons. See the caption for Table IV for further explanations.

Initial state	Final state	Width (MeV)	B.R. (%)
$D_s(1^3P_0)$ 2484	$D_s^*\gamma$	0.00901	0.00407
	$DK$	221	99.8
	Total	221	100
$D_s(1P_1)$ 2549	$D_s\gamma$	0.0152	11.2
	$D_s^*\gamma$	0.00540	3.99
	$D^*K$	0.129	95.3
	Total	0.135	100
$D_s(1P_1')$ 2556	$D_s\gamma$	0.00923	0.00659
	$D_s^*\gamma$	0.00961	0.00687
	$D^*K$	140.	100
	Total	140.	100
$D_s(1^3P_2)$ 2592	$D_s^*\gamma$	0.0189	0.188
	$DK$	9.40	93.4
	$D^*K$	0.545	5.41
	$D_s\eta$	0.105	1.04
	Total	10.07	100

TABLE XXIX: Partial widths and branching ratios for strong decays for the  $2P$  charm-strange mesons. See the caption for Table IV for further explanations.

Initial state	Final state	Width (MeV)	B.R. (%)
$D_s(2^3P_0)$ 3005	$DK$	50.9	35.0
	$D^*K^*$	39.3	27.0
	$D(1P_1)K$	41.9	28.8
	$D_s\eta$	0.602	0.414
	$D_s\eta'$	12.9	8.86
	Total	145.6	100
$D_s(2P_1)$ 3018	$DK^*$	6.54	4.57
	$D^*K$	61.3	42.9
	$D^*K^*$	38.9	27.2
	$D(1^3P_0)K$	4.95	3.46
	$D(1P_1)K$	3.52	2.46
	$D(1P_1')K$	1.29	0.902
	$D(1^3P_2)K$	0.670	0.469
	$D_s\phi$	16.2	11.3
	$D_s^*\eta$	9.65	6.75
Total	143.0	100	
$D_s(2P_1')$ 3038	$DK^*$	32.1	21.7
	$D^*K$	36.5	24.7
	$D^*K^*$	29.7	20.1
	$D(1^3P_0)K$	1.14	0.772
	$D(1P_1)K$	12.2	8.26
	$D(1P_1')K$	3.38	2.29
	$D(1^3P_2)K$	28.4	19.2
	$D_s\phi$	4.15	2.81
	$D_s^*\eta$	0.153	0.104
	Total	147.6	100
$D_s(2^3P_2)$ 3048	$DK$	8.54	6.49
	$DK^*$	20.7	15.7
	$D^*K$	30.8	23.4
	$D^*K^*$	48.9	37.2
	$D(1P_1)K$	2.45	1.86
	$D(1P_1')K$	4.88	3.71
	$D(1^3P_2)K$	5.17	3.93
	$D_s\eta$	3.38	2.57
	$D_s\eta'$	0.504	0.383
	$D_s\phi$	0.275	0.209
	$D_s^*\eta$	5.90	4.49
	Total	131.5	100

TABLE XXX: Partial widths and branching ratios for strong decays for the  $3^3P_0$  and  $3P_1$  charm-strange mesons. See the caption for Table IV for further explanations.

Initial state	Final state	Width (MeV)	B.R. (%)
$D_s(3^3P_0)$ 3412	$DK$	20.3	19.5
	$D^*K^*$	2.90	2.79
	$D(2^1S_0)K$	15.7	15.1
	$D(1^3P_0)K^*$	4.20	4.04
	$D(1P_1)K$	10.1	9.72
	$D(1P_1)K^*$	9.76	9.39
	$D(1P_1')K^*$	11.6	11.2
	$D(1^3P_2)K^*$	0.968	0.931
	$D(1D_2)K$	20.8	20.0
	$D(1D_2')K$	0.282	0.271
	$D_s^*\phi$	4.03	3.88
$D_s(3P_1)$ 3416	$D_s(1P_1)\eta$	2.01	1.93
	Total	103.9	100
	$DK^*$	6.90	4.62
	$D^*K$	13.0	8.71
	$D^*K^*$	2.53	1.70
	$D(2^3S_1)K$	29.7	19.9
	$D(1^3P_0)K$	2.13	1.43
	$D(1P_1)K$	0.558	0.374
	$D(1P_1)K^*$	28.8	19.3
	$D(1P_1')K$	0.396	0.265
	$D(1P_1')K^*$	11.6	7.77
$D(1^3P_2)K$	33.5	22.4	
$D(1^3P_2)K^*$	3.89	2.61	
$D(1^3D_1)K$	1.76	1.18	
$D(1D_2)K$	1.76	1.18	
$D(1^3D_3)K$	1.90	1.27	
$D_s^*\phi$	2.03	1.36	
$D_s(2^3S_1)\eta$	3.25	2.18	
$D_s(1^3P_2)\eta$	3.44	2.31	
Total	149.2	100	

TABLE XXXI: Partial widths and branching ratios for strong decays for the  $3P_1'$  and  $3^3P_2$  charm-strange mesons. See the caption for Table IV for further explanations.

Initial state	Final state	Width (MeV)	B.R. (%)	
$D_s(3P_1')$ 3433	$DK^*$	7.44	6.06	
	$D^*K$	16.4	13.4	
	$D^*K^*$	4.61	3.76	
	$D(2^3S_1)K$	12.0	9.78	
	$D(1^3P_0)K^*$	2.27	1.85	
	$D(1P_1)K$	2.24	1.83	
	$D(1P_1)K^*$	9.77	7.96	
	$D(1P_1')K$	1.49	1.21	
	$D(1P_1')K^*$	10.1	8.23	
	$D(1^3P_2)K$	7.84	6.39	
	$D(1^3P_2)K^*$	10.5	8.56	
	$D(2P_1)K$	1.48	1.21	
	$D(1D_2)K$	7.62	6.21	
	$D(1^3D_3)K$	20.2	16.5	
	$D_s^*\phi$	1.99	1.62	
	$D_s(2^3S_1)\eta$	1.79	1.46	
	$D_s(1^3P_2)\eta$	2.57	2.09	
	Total		122.7	100
	$D_s(3^3P_2)$ 3439	$DK$	2.25	1.63
		$DK^*$	4.36	3.15
$D^*K$		7.53	5.44	
$D^*K^*$		5.37	3.88	
$D(2^1S_0)K$		7.53	5.44	
$D(2^3S_1)K$		16.2	11.7	
$D(1^3P_0)K^*$		2.02	1.46	
$D(1P_1)K$		10.4	7.51	
$D(1P_1)K^*$		4.49	3.24	
$D(1P_1')K$		2.34	1.69	
$D(1P_1')K^*$		9.17	6.62	
$D(1^3P_2)K$		12.9	9.32	
$D(1^3P_2)K^*$		35.4	25.6	
$D(1D_2)K$		1.33	0.961	
$D(1D_2')K$		2.03	1.47	
$D(1^3D_3)K$		3.97	2.87	
$D_s^*\phi$		1.72	1.24	
$D_s(2^1S_0)\eta$		2.21	1.60	
$D_s(2^3S_1)\eta$		2.47	1.78	
$D_s(1P_1)\eta$		1.79	1.29	
$D_s(1^3P_2)\eta$	1.62	1.17		
Total		138.4	100	

TABLE XXXII: Partial widths and branching ratios for strong decays for the  $4^3P_0$  and  $4P_1$  charm-strange mesons. See the caption for Table IV for further explanations.

Initial state	Final state	Width (MeV)	B.R. (%)	
$D_s(4^3P_0)$ 3764	$DK$	10.2	9.76	
	$D^*K^*$	5.10	4.88	
	$D(2^1S_0)K$	7.88	7.54	
	$D(2^3S_1)K^*$	6.97	6.67	
	$D(3^1S_0)K$	5.19	4.97	
	$D(1P_1)K$	6.66	6.37	
	$D(1^3P_2)K^*$	0.942	0.901	
	$D(2P_1)K$	10.9	10.4	
	$D(1^3D_1)K^*$	1.21	1.16	
	$D(1D_2)K$	2.91	2.78	
	$D(1D_2)K^*$	3.76	3.60	
	$D(2D_2)K$	13.1	12.5	
	$D(1F_3)K$	12.7	12.1	
	$D_s(2^3S_1)\phi$	1.59	1.52	
	$D_s(3^1S_0)\eta$	4.27	4.08	
	$D_s(1^3P_2)\phi$	2.00	1.91	
	$D_s(2P_1)\eta$	3.62	3.46	
	$D_s(1D_2)\eta$	1.78	1.70	
	Total		104.5	100
	$D_s(4P_1)$ 3764	$DK^*$	5.35	4.04
$D^*K$		5.01	3.78	
$D^*K^*$		3.79	2.86	
$D(2^3S_1)K$		8.03	6.06	
$D(2^3S_1)K^*$		4.91	3.70	
$D(3^3S_1)K$		16.3	12.3	
$D(1^3P_0)K$		1.79	1.35	
$D(1^3P_2)K$		7.34	5.54	
$D(2^3P_2)K$		28.6	21.6	
$D(1D_2)K^*$		6.81	5.14	
$D(1D_2')K^*$		1.40	1.06	
$D(1^3D_3)K$		15.4	11.6	
$D(2^3D_1)K$		2.79	2.10	
$D(1^3F_4)K$		2.22	1.67	
$D_s(2^3S_1)\phi$		2.28	1.72	
$D_s(2^3P_2)\eta$	2.85	2.15		
$D_s(1^3D_3)\eta$	1.68	1.27		
Total		132.6	100	

TABLE XXXIII: Partial widths and branching ratios for strong decays for the  $4P_1'$  and  $4^3P_2$  charm-strange mesons. See the caption for Table IV for further explanations.

Initial state	Final state	Width (MeV)	B.R. (%)
$D_s(4P_1')$ 3778	$DK^*$	3.89	3.34
	$D^*K$	9.34	8.02
	$D^*K^*$	4.48	3.85
	$D(2^3S_1)K$	7.24	6.22
	$D(2^3S_1)K^*$	2.13	1.83
	$D(3^3S_1)K$	2.95	2.53
	$D(1P_1')K$	1.54	1.32
	$D(1^3P_2)K$	5.05	4.34
	$D(2P_1)K$	2.40	2.06
	$D(2^3P_2)K$	7.70	6.61
	$D(1D_2)K$	1.25	1.07
	$D(1D_2)K^*$	2.70	2.32
	$D(1D_2')K^*$	2.48	2.13
	$D(1^3D_3)K$	3.25	2.79
	$D(1^3D_3)K^*$	3.51	3.01
	$D(2D_2)K$	5.55	4.77
	$D(2^3D_3)K$	10.4	8.93
	$D(1F_3)K$	4.58	3.93
	$D(1^3F_4)K$	12.4	10.6
	$D_s(3^3S_1)\eta$	6.27	5.38
	$D_s(2^3P_2)\eta$	3.62	3.11
	$D_s(1^3D_3)\eta$	1.59	1.37
	Total		116.5
$D_s(4^3P_2)$ 3783	$DK^*$	1.73	1.39
	$D^*K$	2.76	2.22
	$D^*K^*$	7.41	5.97
	$D(2^1S_0)K$	2.09	1.68
	$D(2^3S_1)K$	4.50	3.63
	$D(2^3S_1)K^*$	4.10	3.31
	$D(3^1S_0)K$	5.90	4.76
	$D(3^3S_1)K$	10.2	8.22
	$D(1P_1)K$	2.60	2.10
	$D(1P_1')K$	1.98	1.60
	$D(1^3P_2)K$	3.53	2.85
	$D(1^3P_2)K^*$	2.13	1.72
	$D(2P_1)K$	10.8	8.71
	$D(2P_1')K$	1.26	1.02
	$D(2^3P_2)K$	11.1	8.95
	$D(1D_2)K$	5.36	4.32
	$D(1D_2)K^*$	1.68	1.35
	$D(1D_2')K^*$	1.57	1.27
	$D(1^3D_3)K$	4.94	3.98
	$D(1^3D_3)K^*$	10.6	8.55
	$D(2D_2')K$	2.87	2.31
	$D(2^3D_3)K$	2.20	1.77
	$D(1^3F_4)K$	2.66	2.14
$D_s(2^3S_1)\phi$	3.78	3.05	
$D_s(2P_1)\eta$	2.03	1.64	
$D_s(2^3P_2)\eta$	1.57	1.27	
Total		124.0	100

TABLE XXXIV: Partial widths and branching ratios for strong decays for the  $1D$  charm-strange mesons. See the caption for Table IV for further explanations.

Initial state	Final state	Width (MeV)	B.R. (%)
$D_s(1^3D_1)$ 2899	$DK$	93.2	47.3
	$DK^*$	29.5	15.0
	$D^*K$	50.2	25.5
	$D_s\eta$	17.5	8.88
	$D_s^*\eta$	6.62	3.36
Total		197.2	100
$D_s(1D_2)$ 2900	$DK^*$	93.2	81.0
	$D^*K$	21.1	18.3
	$D_s^*\eta$	0.698	0.606
Total		115.1	100
$D_s(1D_2')$ 2926	$DK^*$	7.92	4.05
	$D^*K$	163	83.4
	$D_s^*\eta$	24.6	12.6
Total		195	100
$D_s(1^3D_3)$ 2917	$DK$	26.5	57.7
	$DK^*$	1.52	3.31
	$D^*K$	15.7	34.2
	$D_s\eta$	1.59	3.46
	$D_s^*\eta$	0.573	1.25
Total		46.0	100

TABLE XXXV: Partial widths and branching ratios for strong decays for the  $2D$  charm-strange mesons. See the caption for Table IV for further explanations.

Initial state	Final state	Width (MeV)	B.R. (%)	
$D_s(2^3D_1)$ 3306	$DK$	29.5	13.9	
	$DK^*$	6.13	2.89	
	$D^*K$	12.2	5.76	
	$D^*K^*$	53.1	25.1	
	$D(2^1S_0)K$	21.8	10.3	
	$D(2^3S_1)K$	11.8	5.57	
	$D(1P_1)K$	34.8	16.4	
	$D(1P'_1)K$	3.28	1.55	
	$D(1^3P_2)K$	21.9	10.3	
	$D_s^*\phi$	3.95	1.87	
	$D_s(2^1S_0)\eta$	3.74	1.77	
	$D_s(1P_1)\eta$	3.94	1.86	
	Total	211.8	100	
	$D_s(2D_2)$ 3298	$DK^*$	21.1	19.8
		$D^*K$	12.1	11.4
$D^*K^*$		26.1	24.5	
$D(2^3S_1)K$		4.09	3.84	
$D(1^3P_0)K$		6.02	5.66	
$D(1P_1)K$		5.68	5.34	
$D(1P'_1)K$		5.47	5.14	
$D(1^3P_2)K$		13.1	12.3	
$D_s^*\eta$		4.02	3.78	
$D_s^*\phi$		4.30	4.04	
Total		106.4	100	
$D_s(2D'_2)$ 3323		$DK^*$	10.6	5.22
	$D^*K$	43.5	21.4	
	$D^*K^*$	31.4	15.5	
	$D(2^3S_1)K$	37.3	18.4	
	$D(1^3P_0)K$	2.63	1.30	
	$D(1P_1)K$	8.06	3.97	
	$D(1P'_1)K$	6.52	3.21	
	$D(1^3P_2)K$	42.4	20.9	
	$D_s^*\phi$	4.33	2.13	
	$D_s(2^3S_1)\eta$	2.79	1.37	
	$D_s(1^3P_2)\eta$	5.91	2.91	
	Total	203.0	100	
$D_s(2^3D_3)$ 3311	$DK^*$	3.95	4.49	
	$D^*K$	3.86	4.39	
	$D^*K^*$	22.2	25.3	
	$D(2^1S_0)K$	5.45	6.20	
	$D(2^3S_1)K$	3.19	3.63	
	$D(1P_1)K$	10.4	11.8	
	$D(1P'_1)K$	9.39	10.7	
	$D(1^3P_2)K$	15.2	17.3	
	$D_s^*\eta$	1.84	2.09	
	$D_s^*\phi$	6.64	7.55	
	$D_s(1P'_1)\eta$	1.43	1.63	
	$D_s(1^3P_2)\eta$	1.21	1.38	
	Total	87.9	100	

TABLE XXXVI: Partial widths and branching ratios for strong decays for the  $3^3D_1$  and  $3D_2$  charm-strange mesons. See the caption for Table IV for further explanations.

Initial state	Final state	Width (MeV)	B.R. (%)
$D_s(3^3D_1)$ 3658	$DK$	12.8	6.45
	$DK^*$	3.76	1.89
	$D^*K$	5.56	2.80
	$D^*K^*$	11.1	5.59
	$D(2^1S_0)K$	8.73	4.40
	$D(2^3S_1)K$	4.48	2.26
	$D(2^3S_1)K^*$	18.1	9.12
	$D(3^1S_0)K$	10.7	5.39
	$D(3^3S_1)K$	3.69	1.86
	$D(1P_1)K$	11.9	6.00
	$D(1^3P_2)K$	4.32	2.18
	$D(1^3P_2)K^*$	21.1	10.6
	$D(2P_1)K$	21.7	10.9
	$D(2P'_1)K$	2.61	1.32
	$D(2^3P_2)K$	12.6	6.35
	$D(1D_2)K$	8.40	4.23
	$D(1^3D_3)K$	9.37	4.72
	$D(1F_3)K$	5.38	2.71
	$D_s(2P_1)\eta$	5.45	2.75
$D_s(1D_2)\eta$	3.81	1.92	
Total	198.5	100	
$D_s(3D_2)$ 3650	$DK^*$	12.1	10.0
	$D^*K$	3.92	3.25
	$D^*K^*$	8.52	7.05
	$D(2^1S_0)K^*$	2.05	1.70
	$D(2^3S_1)K$	7.02	5.81
	$D(2^3S_1)K^*$	14.5	12.0
	$D(1^3P_0)K$	2.65	2.19
	$D(1P_1)K^*$	2.57	2.13
	$D(1P'_1)K$	1.72	1.42
	$D(1^3P_2)K$	7.52	6.23
	$D(1^3P_2)K^*$	11.2	9.27
	$D(2^3P_0)K$	4.2	3.48
	$D(2P_1)K$	4.32	3.58
	$D(2P'_1)K$	3.09	2.56
$D(2^3P_2)K$	8.57	7.10	
$D(1D_2)K$	3.26	2.70	
$D(1^3D_3)K$	8.45	7.00	
$D_s(2^3S_1)\eta$	3.47	2.87	
$D_s(1^3P_2)\eta$	2.05	1.70	
Total	120.8	100	

TABLE XXXVII: Partial widths and branching ratios for strong decays for the  $3D'_2$  and  $3^3D_3$  charm-strange mesons. See the caption for Table IV for further explanations.

Initial state	Final state	Width (MeV)	B.R. (%)	
$D_s(3D'_2)$ 3672	$DK^*$	2.88	1.38	
	$D^*K$	19.3	9.27	
	$D^*K^*$	9.72	4.67	
	$D(2^1S_0)K^*$	11.6	5.57	
	$D(2^3S_1)K$	13.9	6.67	
	$D(2^3S_1)K^*$	15.3	7.34	
	$D(3^3S_1)K$	14.1	6.77	
	$D(1P_1)K^*$	8.24	3.96	
	$D(1P'_1)K$	2.82	1.35	
	$D(1^3P_2)K$	14.1	6.77	
	$D(1^3P_2)K^*$	11.4	5.47	
	$D(2P_1)K$	5.97	2.87	
	$D(2P'_1)K$	3.63	1.74	
	$D(2^3P_2)K$	24.0	11.5	
	$D(1D_2)K$	5.17	2.48	
	$D(1^3D_3)K$	12.4	5.95	
	$D(1^3F_4)K$	7.85	3.77	
	$D_s(2^3P_2)\eta$	7.14	3.43	
	$D_s(1^3D_3)\eta$	4.11	1.97	
	Total		208.3	100
$D_s(3^3D_3)$ 3661	$DK^*$	0.954	0.806	
	$D^*K$	1.43	1.21	
	$D^*K^*$	14.7	12.4	
	$D(2^1S_0)K^*$	5.92	5.00	
	$D(2^3S_1)K$	2.58	2.18	
	$D(2^3S_1)K^*$	17.8	15.0	
	$D(1P_1)K$	1.32	1.11	
	$D(1P_1)K^*$	3.96	3.34	
	$D(1P'_1)K$	3.81	3.22	
	$D(1^3P_2)K$	3.95	3.34	
	$D(1^3P_2)K^*$	10.4	8.78	
	$D(2P_1)K$	7.86	6.64	
	$D(2P'_1)K$	6.33	5.35	
	$D(2^3P_2)K$	9.61	8.11	
	$D(1D_2)K$	5.05	4.26	
	$D(1^3D_3)K$	6.90	5.83	
	$D_s(1^3P_2)\phi$	2.85	2.41	
	Total		118.4	100

TABLE XXXVIII: Partial widths and branching ratios for strong decays for the  $1F$  charm-strange mesons. See the caption for Table IV for further explanations.

Initial state	Final state	Width (MeV)	B.R. (%)	
$D_s(1^3F_2)$ 3208	$DK$	44.8	15.3	
	$DK^*$	33.7	11.5	
	$D^*K$	37.7	12.9	
	$D^*K^*$	29.8	10.2	
	$D(1P_1)K$	97.4	33.3	
	$D(1P'_1)K$	2.53	0.865	
	$D(1^3P_2)K$	13.1	4.48	
	$D_s\eta$	7.90	2.70	
	$D_s\eta'$	3.65	1.25	
	$D_s\phi$	3.28	1.12	
	$D_s^*\eta$	5.33	1.82	
	$D_s(1P_1)\eta$	9.68	3.31	
	Total		292.5	100
$D_s(1F_3)$ 3186	$DK^*$	79.9	43.7	
	$D^*K$	41.2	22.6	
	$D^*K^*$	48.8	26.7	
	$D_s\phi$	6.70	3.67	
	$D_s^*\eta$	2.08	1.14	
	Total		182.6	100
$D_s(1F'_3)$ 3218	$DK^*$	20.2	6.26	
	$D^*K$	93.2	28.9	
	$D^*K^*$	55.9	17.3	
	$D(1P_1)K$	2.49	0.772	
	$D(1^3P_2)K$	123	38.1	
	$D_s^*\eta$	14.1	4.37	
$D_s(1^3P_2)\eta$	$D_s(1^3P_2)\eta$	8.72	2.70	
	Total		323	100
	$D_s(1^3F_4)$ 3190	$DK$	28.8	15.9
		$DK^*$	8.37	4.61
		$D^*K$	24.7	13.6
$D^*K^*$		112	61.7	
Total		182	100	



TABLE XXXIX: Partial widths and branching ratios for strong decays for the  $2^3F_2$  and  $2F_3$  charm-strange mesons. See the caption for Table IV for further explanations.

Initial state	Final state	Width (MeV)	B.R. (%)
$D_s(2^3F_2)$ 3562	$DK$	19.5	7.77
	$DK^*$	10.0	3.98
	$D^*K$	13.7	5.46
	$D^*K^*$	18.6	7.41
	$D(2^1S_0)K$	5.25	2.09
	$D(2^1S_0)K^*$	4.94	1.97
	$D(2^3S_1)K$	6.14	2.45
	$D(1^3P_0)K^*$	4.83	1.92
	$D(1P_1)K$	28.3	11.3
	$D(1P_1)K^*$	9.88	3.94
	$D(1P_1')K$	3.84	1.53
	$D(1P_1')K^*$	7.28	2.90
	$D(1^3P_2)K$	10.9	4.34
	$D(1^3P_2)K^*$	6.91	2.75
	$D(2P_1)K$	36.8	14.7
	$D(2P_1')K$	0.399	0.159
	$D(2^3P_2)K$	4.53	1.80
	$D(1D_2)K$	28.2	11.2
	$D(1^3D_3)K$	8.13	3.24
	$D_s^*\phi$	3.26	1.30
$D_s(1D_2)\eta$	6.25	2.49	
Total		251.0	100
$D_s(2F_3)$ 3540	$DK^*$	24.9	17.7
	$D^*K^*$	16.4	11.6
	$D(2^1S_0)K^*$	7.15	5.07
	$D(2^3S_1)K$	18.5	13.1
	$D(1^3P_0)K$	2.41	1.71
	$D(1^3P_0)K^*$	1.69	1.20
	$D(1P_1)K$	1.38	0.979
	$D(1P_1)K^*$	13.0	9.22
	$D(1P_1')K$	2.98	2.11
	$D(1P_1')K^*$	5.54	3.93
	$D(1^3P_2)K$	21.0	14.9
	$D(1^3P_2)K^*$	9.18	6.51
	$D(1^3D_1)K$	2.48	1.76
	$D(1D_2)K$	3.95	2.80
	$D(1^3D_3)K$	1.67	1.18
	Total		141.0

## V. CLASSIFICATION OF THE OBSERVED CHARM MESONS

The Belle, BaBar and LHCb collaborations have increased our knowledge of charm mesons considerably in recent years which has spawned a large number of theory papers attempting to categorize these new states. We list

TABLE XL: Partial widths and branching ratios for strong decays for the  $2F_3'$  and  $2^3F_4$  charm-strange mesons. See the caption for Table IV for further explanations.

Initial state	Final state	Width (MeV)	B.R. (%)
$D_s(2F_3')$ 3569	$DK^*$	0.815	0.326
	$D^*K$	36.2	14.5
	$D^*K^*$	17.5	6.99
	$D(2^3S_1)K$	13.7	5.47
	$D(1P_1)K^*$	5.04	2.01
	$D(1P_1')K$	3.56	1.42
	$D(1P_1')K^*$	7.73	3.09
	$D(1^3P_2)K$	36.3	14.5
	$D(1^3P_2)K^*$	18.6	7.43
	$D(2^3P_2)K$	41.7	16.7
	$D(1D_2)K$	5.45	2.18
	$D(1^3D_3)K$	34.0	13.6
	$D_s(2^3S_1)\eta$	5.10	2.04
	$D_s(1^3D_3)\eta$	7.24	2.89
Total		250.3	100
$D_s(2^3F_4)$ 3544	$DK$	3.59	2.54
	$D^*K$	0.254	0.179
	$D^*K^*$	32.4	22.9
	$D(2^1S_0)K$	10.8	7.63
	$D(2^3S_1)K$	10.6	7.49
	$D(1^3P_0)K^*$	3.04	2.15
	$D(1P_1)K$	11.2	7.91
	$D(1P_1)K^*$	3.38	2.39
	$D(1P_1')K$	4.94	3.49
	$D(1P_1')K^*$	5.03	3.55
	$D(1^3P_2)K$	10.4	7.35
	$D(1^3P_2)K^*$	29.6	20.9
$D(1D_2')K$	2.90	2.05	
$D(1^3D_3)K$	5.32	3.76	
Total		141.5	100

these new states and their properties in Table XLIV.

The  $1P$  multiplet is well established and its measured properties agree well with theoretical expectations. Theory expects in the heavy quark limit two doublets, the  $j = 1/2$  doublet composed of a  $0^+$  and  $1^+$  state, corresponding to the  $D_0(2400)$  and  $D_1(2430)$  states, that decay via  $S$ -wave and are broad, and the  $j = 3/2$  doublet composed of a  $1^+$  and  $2^+$  state, corresponding to the  $D_1(2420)$  and the  $D_2^*(2460)$  that decay via  $D$ -wave and are relatively narrow. These states have been discussed in the literature (see for example [48]).

It is the large number of newly observed states that concerns us here. Given the success of quark model calculations in describing the  $1P$  states we use the QM predictions of the previous sections to classify these new states. The success of these efforts can be used to gauge the relia-

TABLE XLI: Partial widths and branching ratios for strong decays for the  $1G$  charm-strange mesons. See the caption for Table IV for further explanations.

Initial state	Final state	Width (MeV)	B.R. (%)
$D_s(1^3G_3)$ 3469	$DK$	22.0	6.70
	$DK^*$	20.5	6.24
	$D^*K$	22.3	6.79
	$D^*K^*$	47.4	14.4
	$D(2^1S_0)K$	7.27	2.21
	$D(2^3S_1)K$	3.76	1.15
	$D(1P_1)K$	66.5	20.3
	$D(1P_1)K^*$	16.6	5.06
	$D(1^3P_2)K$	19.6	5.97
	$D(1D_2)K$	65.6	20.0
	$D_s\eta$	3.46	1.05
	$D_s(1P_1)\eta$	9.54	2.91
	Total	328.4	100
	$D_s(1G_4)$ 3436	$DK^*$	45.0
$D^*K$		43.8	23.2
$D^*K^*$		51.0	27.0
$D(1^3P_0)K$		2.51	1.33
$D(1P_1)K$		4.09	2.17
$D(1P_1)K^*$		21.1	11.2
$D(1P_1')K$		2.34	1.24
$D(1^3P_2)K$		4.64	2.46
$D_s\phi$		5.59	2.96
$D_s^*\eta$		2.20	1.17
$D_s^*\phi$		2.87	1.52
Total		188.6	100
$D_s(1G_4')$ 3469		$DK^*$	24.0
	$D^*K$	50.2	14.2
	$D^*K^*$	56.8	16.0
	$D(2^3S_1)K$	10.1	2.85
	$D(1P_1)K$	5.03	1.42
	$D(1^3P_2)K$	92.9	26.2
	$D(1^3P_2)K^*$	9.96	2.81
	$D(1^3D_3)K$	74.9	21.1
	$D_s^*\eta$	6.94	1.96
	$D_s^*\phi$	3.73	1.05
	$D_s(1^3P_2)\eta$	11.9	3.36
	Total	354.5	100
	$D_s(1^3G_5)$ 3433	$DK$	23.1
$DK^*$		10.4	5.77
$D^*K$		24.0	13.3
$D^*K^*$		92.3	51.2
$D(1P_1)K$		3.59	1.99
$D(1P_1')K$		2.91	1.61
$D(1^3P_2)K$		7.31	4.05
$D(1^3P_2)K^*$		5.38	2.98
$D_s^*\phi$		6.10	3.38
Total		180.4	100

TABLE XLII: Partial widths and branching ratios for strong decays for the  $2^3G_3$  and  $2G_4$  charm-strange mesons. See the caption for Table IV for further explanations.

Initial state	Final state	Width (MeV)	B.R. (%)
$D_s(2^3G_3)$ 3789	$DK$	12.4	4.33
	$DK^*$	8.94	3.13
	$D^*K$	11.0	3.85
	$D^*K^*$	6.34	2.22
	$D(2^1S_0)K^*$	6.73	2.35
	$D(2^3S_1)K^*$	13.5	4.72
	$D(3^1S_0)K$	3.30	1.15
	$D(1P_1)K$	22.3	7.80
	$D(1P_1)K^*$	7.74	2.71
	$D(1P_1')K^*$	7.10	2.48
	$D(1^3P_2)K$	5.18	1.81
	$D(1^3P_2)K^*$	14.8	5.17
	$D(2P_1)K$	16.0	5.59
	$D(2^3P_2)K$	8.25	2.88
	$D(1D_2)K$	23.9	8.36
	$D(1D_2)K^*$	16.2	5.66
	$D(1^3D_3)K$	8.63	3.02
$D(2D_2)K$	31.3	10.9	
$D(1F_3)K$	18.5	6.47	
$D_s(2P_1)\eta$	5.15	1.80	
$D_s(1F_3)\eta$	6.52	2.28	
Total	286.0	100	
$D_s(2G_4)$ 3759	$DK^*$	20.3	10.2
	$D^*K$	4.70	2.36
	$D^*K^*$	13.9	6.99
	$D(2^1S_0)K^*$	14.7	7.39
	$D(2^3S_1)K$	21.1	10.6
	$D(2^3S_1)K^*$	14.0	7.04
	$D(1P_1)K^*$	10.5	5.28
	$D(1P_1')K^*$	6.37	3.20
	$D(1^3P_2)K$	17.4	8.75
	$D(1^3P_2)K^*$	10.2	5.13
	$D(2^3P_0)K$	2.07	1.04
	$D(2P_1)K$	3.09	1.55
	$D(2^3P_2)K$	3.35	1.68
$D(1^3D_1)K$	2.86	1.44	
$D(1D_2)K$	3.52	1.77	
$D(1D_2)K^*$	27.2	13.7	
$D(1^3D_3)K$	4.25	2.14	
$D(1^3D_3)K^*$	2.33	1.17	
Total	198.9	100	

TABLE XLIII: Partial widths and branching ratios for strong decays for the  $2G'_4$  and  $2^3G_5$  charm-strange mesons. See the caption for Table IV for further explanations.

Initial state	Final state	Width (MeV)	B.R. (%)
$D_s(2G'_4)$ 3790	$DK^*$	3.65	1.20
	$D^*K$	26.1	8.57
	$D^*K^*$	14.9	4.89
	$D(2^1S_0)K^*$	6.80	2.23
	$D(2^3S_1)K^*$	16.7	5.48
	$D(3^3S_1)K$	4.11	1.35
	$D(1P_1)K^*$	7.61	2.50
	$D(1P'_1)K^*$	6.88	2.26
	$D(1^3P_2)K$	30.6	10.0
	$D(1^3P_2)K^*$	15.5	5.09
	$D(2P_1)K$	3.80	1.25
	$D(2^3P_2)K$	23.8	7.82
	$D(1D_2)K$	4.16	1.37
	$D(1^3D_3)K$	30.3	9.95
	$D(1^3D_3)K^*$	19.5	6.40
	$D(2^3D_3)K$	30.6	10.0
	$D(1^3F_4)K$	21.5	7.06
	$D_s(2^3P_2)\eta$	5.74	1.88
	$D_s(1^3F_4)\eta$	7.21	2.37
	Total		304.5
$D_s(2^3G_5)$ 3757	$DK$	7.33	3.83
	$DK^*$	1.80	0.941
	$D^*K$	3.65	1.91
	$D^*K^*$	33.7	17.6
	$D(2^1S_0)K$	8.90	4.65
	$D(2^1S_0)K^*$	2.39	1.25
	$D(2^3S_1)K$	10.9	5.70
	$D(2^3S_1)K^*$	26.1	13.6
	$D(1P_1)K$	7.03	3.68
	$D(1P_1)K^*$	3.84	2.01
	$D(1P'_1)K^*$	5.13	2.68
	$D(1^3P_2)K$	5.24	2.74
	$D(1^3P_2)K^*$	12.6	6.59
	$D(2P_1)K$	2.72	1.42
	$D(2P'_1)K$	2.69	1.41
	$D(2^3P_2)K$	4.69	2.45
	$D(1D_2)K$	2.24	1.17
	$D(1D'_2)K$	3.87	2.02
	$D(1^3D_3)K$	5.76	3.01
	$D(1^3D_3)K^*$	24.9	13.0
$D_s(1^3P_2)\phi$	3.98	2.08	
Total		191.2	100

bility of our predictions for the properties of undiscovered states. These states have been discussed in numerous papers [16, 17, 20–29, 83, 90–97].

### A. The $D_J(2550)^0$ and $D_J^*(2600)^0$ States

Both the BaBar [2] and LHCb [11] collaborations have reported states around 2550 MeV and 2600 MeV whose measured properties we list in Table XLIV. The only states expected to fall in this mass region are the  $2^1S_0(c\bar{q})$  and  $2^3S_1(c\bar{q})$  states.

Starting with the  $D_J(2550)^0$ , the masses reported by the two experiments are inconsistent at the  $2\sigma$  level. However BaBar and LHCb measure the widths to be 130 MeV and 178 MeV with large errors. Given the large measured widths we believe that the experiments are seeing the same state but that it is difficult to extract masses precisely. With this assumption we average the masses and widths to obtain  $M(D_J(2550)^0) = 2559$  MeV and  $\Gamma(D_J(2550)^0) = 154$  MeV but don't attempt to estimate uncertainties given the naivety of the averaging. In addition LHCb makes the point that extracting its parameters is complicated [11]. Both experiments identify the  $D_J(2550)^0$  as the  $2^1S_0(c\bar{q})$  state. We predict the mass and width of the  $2^1S_0(c\bar{q})$  state to be 2581 MeV and 80 MeV respectively. We note that we predict the  $1^3S_1$  mass to be 2041 MeV which is  $\sim 34$  MeV greater than its observed mass so that if we rescale the  $2^1S_0(c\bar{q})$  mass by this amount we obtain 2547 MeV which is consistent with the observed average value. The calculated width is significantly smaller than the average of the measured widths. However, due to both the uncertainty in the theoretical width predictions and the large uncertainty in the measured width we consider the agreement between theory and experiment to be acceptable and conclude that the  $D_J(2550)^0$  is the  $2^1S_0(c\bar{q})$  state.

We follow the same logic in comparing the measured properties of the  $D_J^*(2600)^0$  to the predicted properties for the  $2^3S_1(c\bar{q})$ . Again the masses reported by BaBar and LHCb for the  $D_J^*(2600)^0$  are incompatible at the level of  $2\sigma$  and the measured widths are 93 and 140 MeV respectively with large errors. Averaging the masses and widths measured by the two experiments we obtain  $M(D_J^*(2600)^0) = 2629$  MeV and  $\Gamma(D_J^*(2600)^0) = 117$  MeV and again we do not assign errors given the lack of justification for using simple averages. We predict the mass and width of the  $2^3S_1(c\bar{q})$  state to be 2643 MeV and 102 MeV respectively. Again, if we rescale the  $2^3S_1(c\bar{q})$  mass down by 34 MeV we obtain 2609 MeV. Further, we find that  $\Gamma(D^*(2S) \rightarrow D\pi)/\Gamma(D^*(2S) \rightarrow D^*\pi) = 0.44$  versus the BaBar [2] measurement of  $0.32 \pm 0.02 \pm 0.09$ . We conclude that the  $D_J^*(2600)^0$  properties are consistent with the predicted properties for the  $2^3S_1(c\bar{q})$ .

To summarize, our results support the identification of the  $D_J(2550)^0$  and  $D_J^*(2600)^0$  with the  $2^1S_0(c\bar{q})$  and  $2^3S_1(c\bar{q})$  respectively made by the BaBar [2] and LHCb [11] collaborations and previous theoretical studies [23–

TABLE XLIV: Recently observed charm mesons. The first uncertainty is statistical, the second uncertainty is due to systematic uncertainties and the third when included is for model dependent uncertainties.

State	$J^P$	Observed Decays	Mass (MeV)	Width (MeV)	References
$D_J(2550)^0$	$0^-$	$D^{*+}\pi^-$	$2539.4 \pm 4.5 \pm 6.8$	$130 \pm 12 \pm 13$	BaBar [2]
$D_J(2580)^0$		$D^{*+}\pi^-$	$2579.5 \pm 3.4 \pm 3.5$	$177.5 \pm 17.8 \pm 46.0$	LHCb [11]
$D_J^*(2600)^0$		$D^+\pi^-$	$2608.7 \pm 2.4 \pm 2.5$	$93 \pm 6 \pm 13$	BaBar [2]
				$\Gamma(\rightarrow D^+\pi^-)/\Gamma(\rightarrow D^{*+}\pi^-) = 0.32 \pm 0.02 \pm 0.09$	BaBar [2]
$D_J^*(2650)^0$		$D^{*+}\pi^-$	$2649.2 \pm 3.5 \pm 3.5$	$140.2 \pm 17.1 \pm 18.6$	LHCb [11]
$D_J(2750)^0$		$D^{*+}\pi^-$	$2752.4 \pm 1.7 \pm 2.7$	$71 \pm 6 \pm 11$	BaBar [2]
$D_J(2740)^0$		$D^{*+}\pi^-$	$2737.0 \pm 3.5 \pm 11.2$	$73.2 \pm 13.4 \pm 25.0$	LHCb [11]
$D_J^*(2760)^0$		$D^{*+}\pi^-$	$2761.1 \pm 5.1 \pm 6.5$	$74.4 \pm 3.4 \pm 37.0$	LHCb [11]
		$D^+\pi^-$	$2760.1 \pm 1.1 \pm 3.7$	$74.4 \pm 3.4 \pm 19.1$	LHCb [11]
		$D^+\pi^-$	$2763.3 \pm 2.3 \pm 2.3$	$60.9 \pm 5.1 \pm 3.6$	BaBar [2]
				$\Gamma(\rightarrow D^+\pi^-)/\Gamma(\rightarrow D^{*+}\pi^-) = 0.42 \pm 0.05 \pm 0.11$	BaBar [2]
$D_J^*(2760)^+$		$D^0\pi^+$	$2771.7 \pm 1.7 \pm 3.8$	$66.7 \pm 6.6 \pm 10.5$	LHCb [11]
$D_1^*(2760)^0$	$1^-$	$D^+\pi^-$	$2781 \pm 18 \pm 11 \pm 6$	$177 \pm 32 \pm 20 \pm 7$	LHCb [9]
$D_3^*(2760)^-$	$3^-$	$\bar{D}^0\pi^-$	$2798 \pm 7 \pm 1 \pm 7$	$105 \pm 18 \pm 6 \pm 23$	LHCb [10] <sup>a</sup>
$D_J(3000)^0$		$D^{*+}\pi^-$	$2971.8 \pm 8.7$	$188.1 \pm 44.8$	LHCb [11]
$D_J^*(3000)^0$		$D^+\pi^-$	$3008.1 \pm 4.0$	$110.5 \pm 11.5$	LHCb [11]

<sup>a</sup>We quote the results from the isobar analysis.

26, 32, 90, 96, 97].

### B. The $D_J(2750)^0$ , $D_1^*(2760)^0$ and $D_3^*(2760)^0$ States

The BaBar [2] and LHCb [9–11] collaborations have observed a number of new states in the mass region of 2740 to 2800 MeV. They can be grouped into the un-natural parity  $D_J(2750)$  seen in the  $D^*\pi$  final state and some number of natural parity states collectively labelled the  $D_J^*(2760)$  which has recently been resolved by LHCb into two states with  $J^P = 1^-$  and  $3^-$  labelled the  $D_1^*(2760)$  [9] and  $D_3^*(2760)$  [10] seen in the  $D\pi$  final state. The states predicted to be closest in mass to these states are the  $1D$  states. The next nearest states are the  $2P$  multiplet which is expected to lie in the 2900 to 2950 MeV mass region but whose quantum numbers are inconsistent with the recent LHCb measurements [9, 10]. We will therefore concentrate on the expected properties of the  $1D$  multiplet. As we did for the  $2S$  multiplet, for the purposes of comparing our mass predictions to the measured masses, we will rescale our predictions down by the difference between predicted and measured masses for the  $D^*(1S)$  state of 34 MeV.

Starting with the  $D_3^*(2760)^0$  state, the measured mass and width from the LHCb isobar analysis are  $2798 \pm 10$  MeV and  $105 \pm 30$  MeV [10] respectively where for simplicity we have combined the statistical, experimental and systematic errors in quadrature. These values should be compared to the predicted mass (after rescaling) and width of the  $1^3D_3(c\bar{q})$  state which are 2799 MeV and 51 MeV respectively. The agreement between experiment and our predictions for both the mass and total width are

satisfactory so we identify the  $D_3^*(2760)^0$  as the  $1^3D_3(c\bar{q})$  state.

Similarly we compare the measured mass and width for the  $D_1^*(2760)^0$  which are  $M = 2781 \pm 22$  MeV and  $\Gamma = 177 \pm 38$  MeV [9] where again we have combined the statistical, experimental and systematic errors in quadrature. The predicted mass (after rescaling) and width are 2774 MeV and 233 MeV respectively which are in good agreement with the measured properties of the  $D_1^*(2760)^0$ . We therefore identify the  $D_1^*(2760)^0$  as the  $1^3D_1(c\bar{q})$  state.

The final state in this mass region is the un-natural parity  $D_J(2750)^0$  state. For the purposes of this discussion we average the BaBar [2] and LHCb [11] measurements to obtain  $M = 2744.7$  MeV and  $\Gamma = 72.1$  MeV. The measured mass is marginally inconsistent with the predicted masses of the two  $J = 2$   $D$ -wave states;  $M(1D_2) = 2782$  and  $M(1D_2') = 2811$  MeV (after rescaling). The predicted widths are  $\Gamma(1D_2) = 105$  MeV and  $\Gamma(1D_2') = 244$  respectively. Considering both the experimental uncertainty, which at least for the LHCb measurement is large, and the theoretical uncertainty, it is reasonable to identify the  $D_J(2750)^0$  with the  $1D_2(c\bar{q})$  state. This identification can be verified by observing the  $D_J(2750)^0$  in other decay modes. For example,  $BR(1D_2 \rightarrow D\rho) = 58\%$  while  $BR(1D_2' \rightarrow D\rho) = 2.4\%$ . This should be a relatively simple state to observe. The second largest decay mode for the  $1D_2'$  is  $BR(1D_2' \rightarrow D^*\pi) \sim 38\%$  vs  $BR(1D_2 \rightarrow D^*\pi) \sim 20\%$ . Finally, the next largest BR for  $1D_2'$  is  $BR(1D_2' \rightarrow D(1^3P_2)\pi) = 37\%$  vs  $BR(1D_2 \rightarrow D(1^3P_2)\pi) < 1\%$ , which is another discriminator between these two possibilities although this final state is likely to be difficult to observe.

We conclude that the  $D_1^*(2760)^0$ ,  $D_3^*(2760)^0$  and  $D_J(2750)^0$  states can be identified with the  $1^3D_1(c\bar{q})$ ,  $1^3D_3(c\bar{q})$  and  $1D_2(c\bar{q})$  quark model states, respectively. Our identification of the  $D_J(2750)^0$  with the  $1D_2(c\bar{q})$  is consistent with other studies [17, 20, 25, 90, 97] although in some cases they label this state with the prime.

With three of the four  $1D$  states observed by the BaBar and LHCb collaborations there is one remaining  $1D$  state to be found. However, with four overlapping states it is not an easy task to disentangle them based solely on mass and total width measurements and to make precise measurements of their properties. Measuring BR's will be useful for solidifying the spectroscopic assignments given above and resolving ambiguities and inconsistencies. For example, the LHCb collaboration resolved the  $D_J^*(2760)$  into  $J = 1$  and  $J = 3$  states. Our calculations predict  $\Gamma(D\pi)/\Gamma(D^*\pi) = 1.8$  for the  $1^3D_1(c\bar{q})$  and 1.3 for  $1^3D_3(c\bar{q})$ . These are inconsistent with the BaBar measurement of  $0.42 \pm 0.05 \pm 0.11$  for the  $D_J^*(2760)^0$  [2]. It is possible that a new measurement will resolve this discrepancy but it is also possible that the  $D^*\pi$  signal contains significant contributions from broad overlapping  $D_2$  states. Further useful information about these states can be obtained by measuring BR's into other final states such as to  $D\rho$  and  $D_s K$  with the relevant BR's given in Table XIII.

### C. The $D_J(3000)^0$ and $D_J^*(3000)^0$ States

LHCb has reported two states around 3000 MeV, the natural parity state  $D_J^*(3000)^0$  with mass = 3008.1  $\pm$  4.0 MeV and width = 110.5  $\pm$  11.5 MeV and the un-natural parity state  $D_J(3000)^0$  with mass = 2971.8  $\pm$  8.7 MeV and width = 188.1  $\pm$  44.8 MeV [11]. Our calculations expect the  $2P$ ,  $3S$  and  $1F$  multiplets to lie in this mass region consisting of the natural parity  $2^3P_2$ ,  $2^3P_0$ ,  $3^3S_1$ ,  $1^3F_4$  and  $1^3F_2$  states and the un-natural parity  $2P'_1$ ,  $2P_1$ ,  $3^1S_0$ ,  $1F'_3$  and  $1F_3$  states. All of these states are expected to have widths in the range of 114 to 270 MeV which, given the theoretical and experimental uncertainties, cannot by themselves be used to rule out any of the possibilities. To help us narrow the possibilities we summarize the predicted properties of the  $2P$ ,  $3S$ , and  $1F$  multiplets in Table XLV. We list BR's for the simpler final states under the assumption that they will be easiest to observe. We also include some final states with larger BR's as they contribute to the total width but expect that in many cases they will be challenging to reconstruct.

Before proceeding we note that LHCb comments that the resonance parameters are strongly correlated to the background parametrization and they don't include the broad  $D_0^*(2420)$  [11]. Thus, one should be cautious in how literally one takes the LHCb values.

Given the general uncertainties of our predictions it is difficult to make definitive spectroscopic assignments for the  $D_J^*(3000)$  and  $D_J(3000)$  states. At best we can

narrow down the possibilities, present our most likely assignment and suggest future measurements that could uniquely identify these states. With this caveat we note that in general our mass predictions tend to overestimate masses of excited states rather than underestimate them. The  $2P$  multiplet lies around 2900 MeV, 100 MeV below the observed masses so we consider it less likely that the  $D_J^*(3000)$  and  $D_J(3000)$  are  $2P$  states.

For the natural parity states, this leaves the  $3^3S_1$ ,  $1^3F_4$  and  $1^3F_2$ . We calculate a total width for the  $1^3F_2$  of 243 MeV versus the measured width of  $110.5 \pm 11.5$  MeV. As we have stated previously, we would not be surprised if our width predictions are off by a factor of two. Nevertheless it is likely that the properties of the  $1^3F_2$  are inconsistent with those of the  $D_J^*(3000)$ . As a final discriminator we consider signal strengths assuming that the state with the largest expected signal strength is the state most likely to first be observed. Signal strengths are a product of the production cross section and final state BR. We surmise that the cross section for orbitally excited states are suppressed compared to states with small orbital angular momentum but we don't know how to accurately calculate the production cross section for charm mesons so only consider the final state BR. The BR's for the two remaining possibilities are  $BR(D_1^*(3^3S_1) \rightarrow D\pi) \simeq 3\%$  vs  $BR(D_4^*(1^3F_4) \rightarrow D\pi) \simeq 12\%$ . On this basis we tentatively identify the  $D_J^*(3000)$  as the  $D_4^*(1^3F_4)$  state but note that this conclusion is based on a number of unsubstantiated assumptions.

The key to confirming this identification will be measuring BR's to other final states and ratios of BR's. Observing the  $D_J^*(3000)$  in the  $D^*\pi$  final state would rule out the  $2^3P_0$ . Measuring the ratio  $R = BR(D^*\pi)/BR(D\pi)$  could narrow down the options. Large ratios would imply the  $2^3P_2$  with  $R \sim 3.4$  or  $3^3S_1$  with  $R \sim 1.7$  while a small ratio would imply the  $1^3F_2$  with  $R \sim 0.8$  and a ratio  $\sim 1$  would imply the  $1^3F_4$ . Undoubtedly the experimental errors will be large to start with and therefore not precise enough, also given the theoretical uncertainties, to narrow down the possibilities to one specific state. For example, the  $1^3F_4$  decays almost half the time to  $D^*\rho$  while the  $3^3S_1$  and  $1^3F_2$  have much smaller BR's to this final state. Finally, the  $1^3F_2$  has a much larger BR to  $D\rho$  than does the  $3^3S_1$ . Thus, observing more final states can either confirm the hypothesis that the  $D_J^*(3000)$  is the  $D_4^*(1^3F_4)$  or direct us to an alternative identification.

We follow the same approach when trying to identify the un-natural parity  $D_J(3000)$  state. We will set aside the  $2P_1$  and  $2P'_1$  as they are likely to be too low in mass. None of the three remaining states can be ruled out based on their total widths, considering both the experimental and theoretical uncertainties. The  $3^1S_0$  mass is closest to the measured mass while the  $1F_3$  and  $1F'_3$  have much larger BR's to the observed  $D^*\pi$  final state. We slightly favour the  $D(3^1S_0)$  identification but more information is needed to make a more informed identification. For example, if the  $D_J(3000)$  were observed in the  $D\rho$  final

TABLE XLV: Properties of the  $2P$ ,  $3S$ , and  $1F$  charm meson multiplets. The predicted masses listed here have been shifted down by 34 MeV, the difference between the predicted and measured  $D^*$  masses. We list BR's of the simplest final states and in some cases final states with the largest BR's. Blank entries represent either forbidden decays or BR's too small to be included.

State	Mass (MeV)	Width (MeV)	Branching Ratios (%)									
			$D\pi$	$D^*\pi$	$D\rho$	$D^*\rho$	$D\omega$	$D^*\omega$	$D_s K$	$D_s^* K$	$D_s K^*$	$D_s^* K^*$
Natural parity states												
$2^3P_2$	2923	114	4.4	15	9.3	23	3.0	8.1	3.2	4.9	0.3	
$2^3P_0$	2897	190	13.4			16.8		5.4	0.4			
$3^3S_1$	3076	103	3.1	5.4	0.8	3.2	0.2	1.3		0.6	0.9	6.3
$1^3F_4$	3079	129	12.2	11.8	3.1	45.7	1.0	14.8	0.8	0.6		1.2
$1^3F_2$	2098	243	9.5	7.6	6.7	6.6	2.2	2.1	3.3	2.1	0.8	0.2
Un-natural parity states												
$2P_1$	2890	125		30.3	2.7	19.3	0.9	6.5		7.2	11.4	
$2P_1'$	2924	212		10.2	8.9	11		3.5		2.1	1.9	
$3^1S_0$	3034	106		4.9		9.3		3.3		2.3	2.2	3.2
$1F_3'$	3109	269		17.2	3.6	11.0	1.2	3.6		5.2		0.4
$1F_3$	3074	126		20	31	20.3	10.2	6.6		0.9	3.3	0.4

state the  $3^1S_0$  would be ruled out. Measuring the ratios of BR's of  $R = BR(D\rho)/BR(D^*\pi)$  would provide a powerful discriminator between the remaining options:  $2P_1$ ,  $2P_1'$ ,  $1F_3$  and  $1F_3'$ . Numerous other final states could be used to help identify the quark model assignment of the  $D_J(3000)$  but are typically more difficult to reconstruct so are unlikely to provide useful input in the near future.

We therefore tentatively identify the  $D_J^*(3000)$  as the  $D_4^*(1^3F_4)$  state and favour the  $D_J(3000)$  as the  $D(3^1S_0)$  state although we do not rule out the  $1F_3$  and  $1F_3'$  assignments. Previous studies have come to the same conclusions [90]. However, Ref. [17] agrees with our identification of the  $D_J^*(3000)$  but suggests that the  $D_J(3000)$  is a  $2P_1$  state, Ref. [23] identifies the  $D_J^*(3000)$  as either the  $D_4^*(1^3F_4)$  or  $D_2^*(1^3F_2)$  and the  $D_J(3000)$  as either the  $D_3(1F_3)$  or  $D_1'(2P_1')$ , and Ref.[21] argues that the  $D_J(3000)$  and  $D_J^*(3000)$  are the  $2P_1$  and  $2^3P_0$  respectively. Still other assignments appear in the literature [20]. Clearly further measurements of other BR's will be needed to settle the issue.

## VI. CLASSIFICATION OF THE OBSERVED CHARM-STRANGE MESONS

We summarize the properties of the recently observed charm-strange mesons in Table XLVI.

### A. The $D_{s_1}^*(2709)^\pm$ , $D_{s_1}^*(2860)^-$ and $D_{s_3}^*(2860)^-$ States

The  $D_{s_1}^*(2709)^\pm$  [3–5, 12] and  $D_{s_J}^*(2860)^-$  [3, 5, 12] were first observed by the Belle [4], BaBar [3, 5] and LHCb [12] collaborations. More recently the LHCb collaboration has measured the properties of the

$D_{s_J}^*(2860)^-$  more precisely and found that it is comprised of two overlapping states, the  $D_{s_1}^*(2860)^-$  and  $D_{s_3}^*(2860)^-$  with  $J^P = 1^-$  and  $3^-$  respectively [13, 14]. With this new information it was argued that the  $D_{s_1}^*(2709)^\pm$  is the  $2^3S_1(c\bar{s})$  state and the  $D_{s_1}^*(2860)^-$  and  $D_{s_3}^*(2860)^-$  are the  $1^3D_1(s\bar{c})$  and  $1^3D_3(s\bar{c})$  states respectively [13–15, 19, 31]. The largest overall discrepancy between theory and experiment is for the ratio  $\Gamma(2^3S_1 \rightarrow D^*K)/\Gamma(2^3S_1 \rightarrow DK)$ . However, it was argued that this discrepancy could be explained by treating the  $D_{s_1}^*(2709)^\pm$  as a mixture of  $2^3S_1(c\bar{s})$  and  $1^3D_1(c\bar{s})$  [24, 29–32, 83, 94, 95, 98] with a relatively small  $2^3S_1 - 1^3D_1$  mixing angle of  $\sim 10^\circ$  [31]. A consequence of this identification is that there are another three excited  $D_s$  states in this mass region to be found; the spin-singlet partner of the  $D_{s_1}^*(2709)^\pm$  is expected to lie  $\sim 60$  MeV lower in mass with  $M(2^1S_0(c\bar{s})) \sim 2650$  MeV, a width of  $\sim 78$  MeV and decaying to  $D^*K$  [31]. The  $J = 2$  states using the predicted  $1D$  mass splittings relative to the  $1^3D_3$  mass give  $M(D_2') \sim 2872$  MeV and  $M(D_2) \sim 2846$  MeV with the partial widths given in Table XLVII which were taken from Ref. [31]. We note that in the HQL we expect one of the  $J = 2$  states to be degenerate with the  $1^3D_3$  and relatively narrow while the other  $J = 2$  state is expected to be degenerate with the  $1^3D_1$  and relatively broad which is consistent with our results. It will be interesting to see what experiment has to say about these states.

### B. The $D_{s_J}(3044)^\pm$ State

The remaining new state is the  $D_{s_J}(3044)^\pm$ . This state has been studied by a number of authors [24, 28, 80, 83, 93, 99]. We start by noting that it has only been seen by one experiment, BaBar [5], albeit with 6.0 standard devi-

TABLE XLVI: The recently observed charm-strange mesons. The first uncertainty is statistical, the second uncertainty is due to experimental systematic effects and the third, when given, is due to model variations.

State	$J^P$	Observed Decays	Mass (MeV)	Width (MeV)	References
$D_{s1}^*(2700)^+$	$1^-$	$D^0 K^+$	$2699^{+14}_{-7}$	$127^{+24}_{-19}$	BaBar [6]
				$\frac{\Gamma(D^* K)}{\Gamma(DK)} = 0.91 \pm 0.13 \pm 0.12$	BaBar [5]
$D_{s1}^*(2700)^+$	$1^-$	$D^+ K^0$ and $D^0 K^+$	$2709.2 \pm 1.9 \pm 4.5$	$115.8 \pm 7.3 \pm 12.1$	LHCb [12]
$D_{sJ}^*(2860)^+$		$DK$ and $D^* K$	$2863.2^{+4.0}_{-2.6}$	$58 \pm 11$	PDG [7]
$D_{sJ}^*(2860)^+$		$DK$ and $D^* K$	$2862 \pm 2^{+5}_{-2}$	$48 \pm 3 \pm 6$	BaBar [5]
				$\frac{\Gamma(D^* K)}{\Gamma(DK)} = 1.10 \pm 0.15 \pm 0.19$	BaBar [5]
$D_{s1}^*(2860)^-$	$1^-$	$\bar{D}^0 K^-$	$2859 \pm 12 \pm 6 \pm 23$	$159 \pm 23 \pm 27 \pm 72$	LHCb [13, 14]
$D_{s3}^*(2860)^-$	$3^-$	$\bar{D}^0 K^-$	$2860.5 \pm 2.6 \pm 2.5 \pm 6.0$	$53 \pm 7 \pm 4 \pm 6$	LHCb [13, 14]
$D_{sJ}(3044)^+$		$D^* K$	$3044 \pm 8^{+30}_{-8}$	$239 \pm 35^{+46}_{-42}$	BaBar [5]

TABLE XLVII: Partial widths for the  $1D_2$  and  $1D_2'$   $c\bar{s}$  mesons calculated using the  $^3P_0$  quark pair creation model from Ref. [31]. The  $1D_2$  and  $1D_2'$  masses listed here and used to calculate the partial widths were obtained by subtracting the predicted splittings from the measured  $1^3D_3$  mass.

State	Property	Predicted (MeV)
$D_s(D_2')$	Mass	2872
	$D_{s2}' \rightarrow D^* K$	159
	$D_{s2}' \rightarrow DK^*$	4.4
	$D_{s2}' \rightarrow D^* K^*$	0
	$D_{s2}' \rightarrow D_s^* \eta$	21
	$\Gamma_{\text{Total}}$	184
$D_s(D_2)$	Mass	2846
	$D_{s2} \rightarrow D^* K$	16
	$D_{s2} \rightarrow DK^*$	58
	$D_{s2} \rightarrow D^* K^*$	0
	$D_{s2} \rightarrow D_s^* \eta$	0.4
	$\Gamma_{\text{Total}}$	75

ation statistical significance. It has only been seen in the  $D^* K$  final state implying it is of unnatural parity;  $0^-, 1^+, 2^-, 3^+, 4^-,$  etc. Of all the states with these quantum numbers the predicted masses for the  $2P_1'$  and  $2P_1$  states are closest to the observed mass, 3038 MeV and 3018 MeV respectively. The  $2P_1$  is expected to have a total width of 143 MeV and a BR to the  $D^* K$  final state of 43% while the  $2P_1'$  is expected to have a total width of 148 MeV with BR to  $D^* K$  of 25%. The experimental error on the width is quite large,  $\sim \pm 55$  MeV and there is considerable theoretical uncertainty on the predicted width which could be up to a factor of 2. As a consequence, the  $D_{sJ}(3044)^\pm$  could be either state. Referring to Table XXIX the  $DK^*$  final state might be a useful discriminator between these two possibilities; the  $2P_1'$  is predicted to have a BR of 22% to  $DK^*$  while for the  $2P_1$  it is predicted to be 5%. Another possibility is that because the states are relatively close together and broad, per-

haps BaBar observed two overlapping states. A means of discriminating between these possibilities is to measure BR's to different final states. For example, we estimate that the branching ratios of the  $D_{s1}(2P_1')$  to  $DK^*$  and  $D_s \phi$  are 22% and 2.8% respectively versus 43% and 11.3% respectively for the  $D_{s1}(2P_1)$ . Measurement of BR's to these final states would provide a good discriminator for these possibilities (see also Ref. [24, 80, 83, 99]). A final possibility is that the observed state does decay to  $DK$  but that it simply was not observed. The  $D_{s2}^*(2^3P_2)$  state is predicted to have a mass  $\sim 3048$  MeV, total width 132 MeV with BR's to  $D^* K$  and  $DK$  of 23% and 6.5% respectively. It may have been that the signal in the  $DK$  final state was simply too small to see with limited statistics.

While we consider it most likely that the  $D_{sJ}(3044)^\pm$  is a member of the  $2P(c\bar{s})$  multiplet we mention other possibilities for completeness. Other unnatural parity states with masses not too far from the  $D_{sJ}(3044)^\pm$  are the  $1F_3$  with  $M = 3186$  MeV and  $\Gamma = 183$  MeV, the  $1F_3'$  with  $M = 3218$  MeV and  $\Gamma = 323$  MeV, the  $2D_2$  with  $M = 3298$  MeV and  $\Gamma = 106$  MeV and the  $2D_2'$  with  $M = 3323$  MeV and  $\Gamma = 203$  MeV. However we consider all of these possibilities unlikely as the predicted masses are over 100 MeV from the observed mass. And although it would not surprise us if our predictions were off by several tens of MeV we do not expect them to be off by over 100 MeV. A final possibility is the  $3^1S_0$  with  $M = 3154$  MeV and  $\Gamma = 79$  MeV with BR to  $D^* K$  of 15%. In this case the predicted width is smaller by a factor of three so that it seems unlikely that the  $D_{sJ}(3044)^\pm$  could be identified as the  $3^1S_0$ .

To summarize, with the information we currently have for the  $D_{sJ}(3044)^\pm$  it is most likely either the  $D_{s1}(2P_1')$  or the  $D_{s1}(2P_1)$  or both states overlapping. This conclusion is consistent with other studies [17, 24, 80, 82, 83, 93, 99]. Another possibility is that it is  $D_{s2}^*(2^3P_2)$  with the signal for the  $DK$  final state too small to be observed with current statistics. These different possibilities can be tested by measuring BR's to  $DK^*$  and  $D_s \phi$  final states. We also expect that it should be possible to observe the  $2P$  partners which will lie in this mass region in  $DK$  and

$D^*K^*$  final states.

## VII. FINDING THE MISSING CHARM MESONS

The key to observing missing states is that their total width is not too large and that the BR's to at least some simple final states are not too small. This is how the new charm states were found by the BaBar and LHCb collaborations. Thus, we can use our tables of charm meson properties to identify candidate states that could be observed in the near future. As the states become more massive, more and more channels open up so that the BR's to easier to observe final states become smaller and smaller. For masses above around 3500 MeV for charm mesons the BR's to simple final states are less than 1% and are likely too small to observe. For charm-strange mesons, BR's to at least some simple final states remain non negligible for all states we consider due to the smaller phase space because of the larger kaon mass relative to that of the pion. Another consideration is that states within multiplets will be overlapping and states in different multiplets are close enough in mass that it will require more than "bump hunting" to classify newly found states. Determining the spin of a state and measuring BR's to multiple final states will be important to disentangle the spectrum. We have already seen examples of this in the preceding sections.

### A. The Charm Mesons

For the most part, the recently observed states are the states with large BR's to simple final states. For example the predicted BR's of the  $2^3S_1$  and  $2^1S_0$  to the observed final state  $D^*\pi$  are 58% and 99% respectively. Likewise the  $1D$  states have BR's to  $D^*\pi$  ranging from 13% to 38% and the  $1^3F_4$  has a BR to  $D\pi$  of 12%. We will use BR's to simple final states to identify good candidates for discovery.

We start with the  $1D$  multiplet. Three of the states have been observed, the  $1^3D_1$  and  $1^3D_3$  and tentatively the  $1D_2$  leaving only the  $1D'_2$  to be found. This state has a BR of 38% to  $D^*\pi$  but is predicted to be rather broad,  $\sim 240$  MeV, making it potentially difficult to disentangle from the other three  $1D$  states in that mass region. This state might also be seen in the  $D_s^*K$  final state.

We tentatively identified the  $3^1S_0$  state with the  $D_J(3000)$  although the  $1F_3$  and  $1F'_3$  are also possibilities. If we accept the  $3^1S_0$  assignment we would expect that the  $3^3S_1$  should also be seen with comparable statistics. The distinguishing feature is that the  $3^3S_1$  should be seen in both  $D\pi$  and  $D^*\pi$  final states. Even if the  $D_J(3000)$  turns out to be the  $1F_3$  or  $1F'_3$  we expect that the  $3S$  states could be seen in the near future.

The  $2P$  states also have relatively large BR's to  $D^*\pi$  and  $D\pi$  final states. Their masses are expected to be in

the 2900-2950 MeV mass range with widths ranging from 114 to 212 MeV. In fact, some have argued that the  $2^3P_0$  can be identified with the  $D_J^*(3000)$ . We expect that the  $2P$  multiplet can be observed in  $D^*\pi$  and  $D\pi$  final states. The four states are only split by 37 MeV so that it will require the measurement into different final states to uniquely identify the individual states. As we pointed out previously, in addition to  $D^*\pi$  and  $D\pi$ , the  $D\rho$  final state will be a useful discriminator. Other final states which would help are the  $D_sK$ ,  $D_s^*K$ ,  $D_sK^*$  and  $D^*\rho$  although in some cases they only have a sizeable BR for one of the  $2P$  states. In this case their observation in one of these final states would eliminate other possibilities.

The  $1F$  multiplet is next in line using this criteria for "discoverability" with BR's to  $D\pi$  and  $D^*\pi$  ranging from 8 to 20%. Their masses are around 3100 MeV with predicted widths ranging from 126 to 270 MeV. Depending on the reliability of our width predictions, the two broad states, the  $1^3F_2$  and  $1F'_3$ , are likely too broad to be easily seen. We have tentatively identified the  $1^3F_4$  with the  $D_J^*(3000)$  state leaving the  $1F_3$  to be found. If found, it is expected to have a large BR into  $D\rho$  which could be used as confirmation.

The  $1G$  multiplet also has a significant BR to the  $D\pi$  and  $D^*\pi$  final states ranging from 4% to 17% depending on the state. Their masses range from around 3360 to 3400 MeV and their widths range from 118 to 254 MeV. The narrower widths correspond to the  $j = 9/2$  doublet and the broader widths to the  $j = 7/2$  doublet. We expect it more likely that the narrower  $1^3G_5$  and  $1G_4$  states will be observed first. The natural parity  $1^3G_5$  decays to both  $D\pi$  and  $D^*\pi$  while the un-natural  $1G_4$  can only decay to  $D^*\pi$ . Other decay modes that can be used to distinguish between these states are  $D\rho$  where  $BR(D(1^3G_5) \rightarrow D\rho) \simeq 3\%$  versus  $BR(D(1G_4) \rightarrow D\rho) \simeq 15\%$  and  $D^*\rho$  where  $BR(D(1^3G_5) \rightarrow D^*\rho) \simeq 32\%$  versus  $BR(D(1G_4) \rightarrow D^*\rho) \simeq 17\%$ . One could use similar measurements to identify the  $1G'_4$  and  $1^3G_3$ .

Beyond these multiplets, the BR's to  $D\pi$  and  $D^*\pi$  final states for the most part become relatively small and other final states will become more important for finding higher excited missing states. We already suggested that the  $D\rho$  and  $D^*\rho$  final states would be useful for identifying excited charm states and for many of the higher excited states they have the largest BR's and could prove crucial for their discovery. For example, in the  $2D$  multiplet  $BR(2^3D_1 \rightarrow D\pi) \simeq 5.1\%$  but  $BR(2^3D_1 \rightarrow D^*\rho) \simeq 13.9\%$ . The challenge is that the  $D^*$  and  $\rho$  will have to be reconstructed with numerous pions in the final state. Similarly,  $BR(2^3D_3 \rightarrow D^*\rho) \simeq 11.4\%$  versus  $BR(2^3D_3 \rightarrow D^*\pi) \simeq 3.0\%$  and  $BR(2D_2 \rightarrow D^*\rho) \simeq 14.7\%$  versus  $BR(2D_2 \rightarrow D^*\pi) \simeq 9.5\%$ . To complete the multiplet we note that  $BR(2D'_2 \rightarrow D^*\rho) \simeq 7.3\%$  versus  $BR(2D'_2 \rightarrow D^*\pi) \simeq 7.8\%$  so that the ratio  $BR(2D_2^{(\prime)} \rightarrow D^*\rho)/BR(2D_2^{(\prime)} \rightarrow D^*\pi)$  could be useful for discriminating between  $2D'_2$  and  $2D_2$ .

One can continue this exercise by examining the predicted BR's of higher mass multiplets given in Tables V-



XXIV. Further examples that satisfy the criteria of being not too broad while having a not too small BR to a simple final state like  $D\pi$  and  $D^*\pi$  are members of the  $2D$  and  $3P$  multiplets etc. The interested reader can identify more candidate states that might be found in the near future by examining Tables V-XXIV.

### B. The Charm-strange Mesons

We will follow the approach used in the previous section to identify likely charm-strange discovery candidates using the criteria that states with large branching ratios to simple final states are the ones most likely to be observed.

The charm-strange states that have recently been observed by Belle, BaBar and LHCb all follow this pattern of large BR's to simple states. For example, the  $D_{s1}^*(2709)$  identified as the  $D_s^*(2^3S_1)$  is predicted to have  $BR(D_s^*(2^3S_1) \rightarrow D^*K) \simeq 58.6\%$  and  $BR(D_s^*(2^3S_1) \rightarrow DK) \simeq 32.5\%$ , the discovery channels. Similarly the  $D_{s1}^*(2860)$  and  $D_{s3}^*(2860)$  are identified as the  $D_s^*(1^3D_1)$  and  $D_s^*(1^3D_3)$  which are predicted to have BR's to  $DK$ , the channel studied by LHCb, of 47.3% and 57.7% respectively. Finally, we tentatively identify the  $D_{sJ}(3044)$  as either  $2P_1$  or  $2P_1'$  whose calculated BR's to  $D^*K$ , the BaBar discovery channel, are 42.9% and 24.7% respectively. The common thread is that all of the recently discovered  $D_{sJ}^*$  have large BR's to simple final states.

If we extrapolate this to other excited states we can expect many more  $D_{sJ}^*$  to be discovered in the near future. The singlet partner of the  $D_{s1}^*(2709)$ , the  $D_s(2^1S_0)$ , is expected to lie 59 MeV lower at 2650 MeV with a width of 74 MeV and a BR of almost 100% to  $D^*K$ . The  $J = 2$  partners of  $D_{s1}^*(2860)$  and  $D_{s3}^*(2860)$  are the  $1D_2$  and  $1D_2'$ , which should lie very close in mass to the  $D_{s1}^*$  and  $D_{s3}^*$ . Their widths are expected to be 115 and 195 MeV respectively with BR's to  $D^*K$  of 18.3% and 83.4%. Finally, if the  $D_{sJ}(3044)$  is the  $2P_1$  or  $2P_1'$  there will be three other  $2P$  partner states, the  $2^3P_2$ ,  $2^3P_0$ , and the other  $J = 1$  state. Because we did not determine if the  $D_{sJ}(3044)$  is the  $2P_1$  or  $2P_1'$  we will make a few comments about all four of the  $2P$  states and refer to Table XXIX for details. All four of the  $2P$  states are close in mass ranging from 3005 MeV for the  $2^3P_0$  to 3048 MeV for the  $2^3P_2$  state. The widths of all four states are around 130-150 MeV. What distinguishes them are their BR's to different final states:  $D_s^*(2^3P_0)$  decays to  $DK$  with  $BR \simeq 35\%$  but does not decay to  $D^*K$ , while the  $D_s(2P_1)$  and  $D_s(2P_1')$  decay to  $D^*K$  with  $BR \simeq 42.9\%$  and 24.7% respectively but do not decay to  $DK$ , and  $D_s^*(2^3P_2)$  can decay to both  $DK$  and  $D^*K$  with BR's of 6.5% and 23.4% respectively. The point is that all of these states have sizeable BR's to final states that have already lead to the observation of a new state in this mass region so that we expect that the remaining three states should also be seen.

So far we have only discussed charm-strange mesons

that are members of multiplets with states that have already been observed. The next most promising states to find are likely to be members of the  $1F$  multiplet and in fact the  $1F_3$  states are alternative possibilities for the  $D_{sJ}(3044)$ . We leaned towards the  $2P_1$  identification primarily because the predicted mass was closer to the observed mass. In any case the  $1F$  states are expected to sit around 3200 MeV. The  $1^3F_4$  is predicted to have a width of 182 MeV with BR's to  $DK$  and  $D^*K$  of 15.9% and 13.6% respectively, the  $1F_3$  and  $1F_3'$  have widths of 183 MeV and 323 MeV respectively with BR's to  $D^*K$  of 22.6% and 28.9% respectively and do not decay to  $DK$ , and the  $1^3F_2$  is predicted to have a width of 292 MeV and decays to  $DK$  and  $D^*K$  with BR's of 15.3% and 12.9% respectively. Although the BR's are all sizeable, the  $1F$  states are expected to be relatively broad so it is not clear if they will be observed in the near future. However, as we have repeatedly pointed out, our width predictions can easily be off by up to a factor of two so that if they turn out to be narrower than we predict, their observation would be more likely.

We note that the  $1G$  multiplet has similar BR's to final states (see Table XLI) as the  $1F$  multiplet so it might also be possible to observe these states with the same caveat regarding their large total widths. It would be extremely interesting to find these states as we would then have a series of angular momentum states stretching from  $L = 0$  to  $L = 4$  which would test the linearity of the Regge trajectory and thus the linearity of the confining potential [45]. If large deviations were found it would also provide some insights into the importance of meson loop contributions to the mass of excited states.

Beyond these states there are a smattering of states that have large BR's to the  $DK$  and  $D^*K$  final states we have focused on. A few examples are: the  $3^3P_0$  with a predicted mass of 3412 MeV, width of 104 MeV and BR to  $DK$  of 19.5%, the  $4^3P_0$  with  $M = 3764$  MeV,  $\Gamma = 105$  MeV and BR to  $DK$  of 10%, the  $2D_2$  with  $M = 3298$  MeV,  $\Gamma = 106$  MeV and BR to  $D^*K$  of 11.4% and the  $2D_2'$  with  $M = 3323$  MeV,  $\Gamma = 203$  MeV and BR to  $D^*K$  of 21.4%. One can turn to Tables XXXI-XLIII to explore further possibilities. As more measurements are made we will be able to gauge the reliability of our predictions and those of others and refine the models to improve their predictive power.

## VIII. SUMMARY

In this paper we calculated the properties of charm and charm-strange mesons using the relativized quark model to calculate masses and wavefunctions which were used to calculate radiative transition partial widths. We calculated hadronic widths using the quark pair creation model with simple harmonic oscillator wavefunctions with the oscillator parameters fitted to the rms radius of the relativized quark model wavefunctions.

We used our results to identify recently observed charm

and charm-strange mesons in terms of quark model spectroscopic states. Our results support the previously made assignment of the  $D_J(2550)^0$  and  $D_J^*(2600)^0$  as the  $2^1S_0(c\bar{q})$  and  $2^3S_1(c\bar{q})$  states respectively. We identify the  $D_1^*(2760)^0$  and  $D_3^*(2760)^0$  as the  $1^3D_1(c\bar{q})$  and  $1^3D_3(c\bar{q})$  respectively and tentatively identify the  $D_J(2750)^0$  as the  $1D_2(c\bar{q})$  state. In the latter case further measurements are needed to strengthen the assignment. We suggested that measurements of BR's to  $D\rho$  and  $D^*\pi$  would be useful. We tentatively identified the  $D_J^*(3000)^0$  as the  $D_4^*(1^3F_4)$  state and favour the  $D_J(3000)^0$  to be the  $D(3^1S_0)$  although we do not rule out the  $1F_3$  and  $1F_3'$  assignments. For the recently observed charm-strange mesons we identify the  $D_{s1}^*(2709)^\pm$ ,  $D_{s1}^*(2860)^-$ , and  $D_{s3}^*(2860)^-$  as the  $2^3S_1(c\bar{s})$ ,  $1^3D_1(s\bar{c})$ , and  $1^3D_3(s\bar{c})$  respectively and suggest that the  $D_{sJ}(3044)^\pm$  is most likely the  $D_{s1}(2P_1)$  or  $D_{s1}(2P_1)$  although it might be the  $D_{s2}^*(2^3P_2)$  with the  $DK$  final state too small to be observed with current statistics.

Finally we suggested excited charm and charm-strange mesons that might be seen in the near future based on the criteria that they do not have too large a total width and they have a reasonable branching ratio to simple final states. We expect that our results comprised of tables of masses, widths and BR's will be useful to this end.

While we have shown the usefulness of our results in identifying newly discovered states we are equally keen that they be a useful guide for future searches for missing states.

### Acknowledgments

This research was supported in part by the Natural Sciences and Engineering Research Council of Canada under grant number 121209-2009 SAPIN.

- 
- [1] A. J. Bevan *et al.* [BaBar and Belle Collaborations], “The Physics of the  $B$  Factories,” *Eur. Phys. J. C* **74**, no. 11, 3026 (2014) [arXiv:1406.6311 [hep-ex]].
- [2] P. del Amo Sanchez *et al.* [BaBar Collaboration], “Observation of new resonances decaying to  $D\pi$  and  $D^*\pi$  in inclusive  $e^+e^-$  collisions near  $\sqrt{s} = 10.58$  GeV,” *Phys. Rev. D* **82**, 111101 (2010) [arXiv:1009.2076 [hep-ex]].
- [3] B. Aubert *et al.* [BaBar Collaboration], “Observation of a New  $D_s$  Meson Decaying to  $DK$  at a Mass of 2.86 GeV/ $c^2$ ,” *Phys. Rev. Lett.* **97**, 222001 (2006) [hep-ex/0607082].
- [4] J. Brodzicka *et al.* [Belle Collaboration], “Observation of a new  $D_{sJ}$  meson in  $B^+ \rightarrow \bar{D}^0 D^0 K^+$  decays,” *Phys. Rev. Lett.* **100**, 092001 (2008) [arXiv:0707.3491 [hep-ex]].
- [5] B. Aubert *et al.* [BaBar Collaboration], “Study of  $D_{sJ}$  decays to  $D^*K$  in inclusive  $e^+e^-$  interactions,” *Phys. Rev. D* **80**, 092003 (2009) [arXiv:0908.0806 [hep-ex]].
- [6] J. P. Lees *et al.* [BaBar Collaboration], “Dalitz plot analyses of  $B^0 \rightarrow D^- D^0 K^+$  and  $B^+ \rightarrow \bar{D}^0 D^0 K^+$  decays,” *Phys. Rev. D* **91**, no. 5, 052002 (2015) [arXiv:1412.6751 [hep-ex]].
- [7] K. A. Olive *et al.* [Particle Data Group Collaboration], “Review of Particle Physics,” *Chin. Phys. C* **38**, 090001 (2014).
- [8] D. Besson *et al.* [CLEO Collaboration], “Observation of a Narrow Resonance of Mass 2.46 GeV/ $c^2$  Decaying to  $D_s^{*+}\pi^0$  and Confirmation of the  $D_{sJ}^*(2317)$  State,” *Phys. Rev. D* **68**, 032002 (2003) [Erratum-ibid. *D* **75**, 119908 (2007)] [hep-ex/0305100].
- [9] R. Aaij *et al.* [LHCb Collaboration], “First observation and amplitude analysis of the  $B^- \rightarrow D^+ K^- \pi^-$  decay,” *Phys. Rev. D* **91**, no. 9, 092002 (2015) [arXiv:1503.02995 [hep-ex]].
- [10] R. Aaij *et al.* [LHCb Collaboration], “Dalitz plot analysis of  $B^0 \rightarrow \bar{D}^0 \pi^+ \pi^-$  decays,” arXiv:1505.01710 [hep-ex].
- [11] R. Aaij *et al.* [LHCb Collaboration], “Study of  $D_J$  meson decays to  $D^+ \pi^-$ ,  $D^0 \pi^+$  and  $D^{*+} \pi^-$  final states in pp collision,” *JHEP* **1309**, 145 (2013) [arXiv:1307.4556].
- [12] R. Aaij *et al.* [LHCb Collaboration], “Study of  $D_{sJ}$  decays to  $D^+ K_S$  and  $D^0 K^+$  final states in  $pp$  collisions,” *JHEP* **1210**, 151 (2012) [arXiv:1207.6016 [hep-ex]].
- [13] R. Aaij *et al.* [LHCb Collaboration], “Observation of overlapping spin-1 and spin-3  $\bar{D}^0 K^-$  resonances at mass 2.86 GeV/ $c^2$ ,” arXiv:1407.7574 [hep-ex].
- [14] R. Aaij *et al.* [LHCb Collaboration], “Dalitz plot analysis of  $B_s^0 \rightarrow \bar{D}^0 K^- \pi^+$  decays,” *Phys. Rev. D* **90**, no. 7, 072003 (2014) [arXiv:1407.7712 [hep-ex]].
- [15] Z. G. Wang, “ $D_{s3}^*(2860)$  and  $D_{s1}^*(2860)$  as the 1D  $c\bar{s}$  states,” *Eur. Phys. J. C* **75**, no. 1, 25 (2015) [arXiv:1408.6465 [hep-ph]].
- [16] P. Colangelo, F. De Fazio and S. Nicotri, “ $D_{sJ}(2860)$  resonance and the  $s_\ell^P = 5/2^- c\bar{s}(c\bar{q})$  doublet,” *Phys. Lett. B* **642**, 48 (2006) [hep-ph/0607245].
- [17] L. Y. Xiao and X. H. Zhong, “Strong decays of higher excited heavy-light mesons in a chiral quark model,” *Phys. Rev. D* **90**, no. 7, 074029 (2014) [arXiv:1407.7408 [hep-ph]].
- [18] H. W. Ke, J. H. Zhou and X. Q. Li, “Study on radiative decays of  $D_{sJ}^*(2860)$  and  $D_{s1}^*(2710)$  into  $D_s$  by means of LFM,” *Eur. Phys. J. C* **75**, no. 1, 28 (2015) [arXiv:1411.0376 [hep-ph]].
- [19] Q. T. Song, D. Y. Chen, X. Liu and T. Matsuki, “ $D_{s1}^*(2860)$  and  $D_{s3}^*(2860)$ : candidates for 1D charmed-strange mesons,” *Eur. Phys. J. C* **75**, no. 1, 30 (2015) [arXiv:1408.0471 [hep-ph]].
- [20] Q. T. Song, D. Y. Chen, X. Liu and T. Matsuki, “Higher radial and orbital excitations in the charmed meson family,” *Phys. Rev. D* **92**, no. 7, 074011 (2015) [arXiv:1503.05728 [hep-ph]].
- [21] Y. Sun, X. Liu and T. Matsuki, “Newly observed  $D_J(3000)^{+,0}$  and  $D_J^*(3000)^0$  as 2P states in  $D$  meson family,” *Phys. Rev. D* **88**, no. 9, 094020 (2013) [arXiv:1309.2203 [hep-ph]].
- [22] B. Zhang, X. Liu, W. -Z. Deng and S. -L. Zhu, “ $D_s J(2860)$  and  $D_s J(2715)$ ,” *Eur. Phys. J. C* **50**, 617 (2007) [hep-ph/0609013].
- [23] G. L. Yu, Z. G. Wang, Z. Y. Li and G. Q. Meng, “Sys-

- tematic analysis of the  $D_J(2580)$ ,  $D_J^*(2650)$ ,  $D_J(2740)$ ,  $D_J^*(2760)$ ,  $D_J(3000)$  and  $D_J^*(3000)$  in  $D$  meson family,” *Chin. Phys. C* **39**, no. 6, 063101 (2015) [arXiv:1402.5955 [hep-ph]].
- [24] D. M. Li, P. F. Ji and B. Ma, “The newly observed opencharm states in quark model,” *Eur. Phys. J. C* **71**, 1582 (2011) [arXiv:1011.1548 [hep-ph]].
- [25] Z. G. Wang, “Analysis of strong decays of the charmed mesons  $D(2550)$ ,  $D(2600)$ ,  $D(2750)$  and  $D(2760)$ ,” *Phys. Rev. D* **83**, 014009 (2011) [arXiv:1009.3605 [hep-ph]].
- [26] Z. G. Wang, “Analysis of strong decays of the charmed mesons  $D_J(2580)$ ,  $D_J^*(2650)$ ,  $D_J(2740)$ ,  $D_J^*(2760)$ ,  $D_J(3000)$ ,  $D_J^*(3000)$ ,” *Phys. Rev. D* **88**, no. 11, 114003 (2013) [arXiv:1308.0533 [hep-ph]].
- [27] E. van Beveren and G. Rupp, “Comment on ‘Study of  $D_{sJ}$  decays to  $D^*K$  in inclusive  $e^+e^-$  interactions’,” *Phys. Rev. D* **81**, 118101 (2010) [arXiv:0908.1142 [hep-ph]].
- [28] A. M. Badalian and B. L. G. Bakker, “Higher excitations of the  $D$  and  $D_s$  mesons,” *Phys. Rev. D* **84**, 034006 (2011) [arXiv:1104.1918 [hep-ph]].
- [29] F. E. Close, C. E. Thomas, O. Lakhina and E. S. Swanson, “Canonical interpretation of the  $D(sJ)(2860)$  and  $D(sJ)(2690)$ ,” *Phys. Lett. B* **647**, 159 (2007) [hep-ph/0608139].
- [30] S. Godfrey and I. T. Jardine, “Comment on the Nature of the  $D_{s1}^*(2710)$  and  $D_{sJ}^*(2860)$  Mesons,” *Phys. Rev. D* **89**, 074023 (2014) [arXiv:1312.6181 [hep-ph]].
- [31] S. Godfrey and K. Moats, “The  $D_{sJ}^*(2860)$  Mesons as Excited D-wave  $c\bar{s}$  States,” *Phys. Rev. D* **90**, no. 11, 117501 (2014) [arXiv:1409.0874 [hep-ph]] [erratum:].
- [32] B. Chen, L. Yuan and A. Zhang, “Possible 2S and 1D charmed and charmed-strange mesons,” *Phys. Rev. D* **83**, 114025 (2011) [arXiv:1102.4142 [hep-ph]].
- [33] G. Moir, M. Peardon, S. M. Ryan, C. E. Thomas and L. Liu, “Excited spectroscopy of charmed mesons from lattice QCD,” *JHEP* **1305**, 021 (2013) [arXiv:1301.7670 [hep-ph]].
- [34] R. Lewis and R. M. Woloshyn, “S and P wave heavy light mesons in lattice NRQCD,” *Phys. Rev. D* **62**, 114507 (2000) [hep-lat/0003011].
- [35] K. Cichy, M. Kalinowski and M. Wagner, “Mass spectra of mesons containing charm quarks - continuum limit results from twisted mass fermions,” *PoS LATTICE 2015*, 093 (2015) [arXiv:1510.07862 [hep-lat]].
- [36] A. De Rujula, H. Georgi and S. L. Glashow, “Charm Spectroscopy Via Electron - Positron Annihilation,” *Phys. Rev. Lett.* **37**, 785 (1976).
- [37] J. L. Rosner, “P Wave Mesons With One Heavy Quark,” *Comments Nucl. Part. Phys.* **16**, 109 (1986).
- [38] N. Isgur and M. B. Wise, “Spectroscopy With Heavy Quark Symmetry,” *Phys. Rev. Lett.* **66**, 1130 (1991).
- [39] E. J. Eichten, C. T. Hill and C. Quigg, “Properties of orbitally excited heavy - light mesons,” *Phys. Rev. Lett.* **71**, 4116 (1993) [arXiv:hep-ph/9308337].
- [40] M. Lu, M. B. Wise and N. Isgur, “Heavy quark symmetry and  $D1(2420) \rightarrow D^* \pi$  decay,” *Phys. Rev. D* **45**, 1553 (1992).
- [41] S. Godfrey and R. Kokoski, “The Properties of p Wave Mesons with One Heavy Quark,” *Phys. Rev. D* **43**, 1679 (1991).
- [42] S. Godfrey and N. Isgur, “Mesons in a Relativized Quark Model with Chromodynamics,” *Phys. Rev. D* **32**, 189 (1985).
- [43] L. Micu, “Decay rates of meson resonances in a quark model,” *Nucl. Phys. B* **10**, 521 (1969).
- [44] A. Le Yaouanc, L. Oliver, O. Pene and J. C. Raynal, “Naive quark pair creation model of strong interaction vertices,” *Phys. Rev. D* **8**, 2223 (1973).
- [45] S. Godfrey, “High Spin Mesons in the Quark Model,” *Phys. Rev. D* **31**, 2375 (1985).
- [46] S. Godfrey and N. Isgur, “Isospin Violation In Mesons And The Constituent Quark Masses,” *Phys. Rev. D* **34**, 899 (1986).
- [47] S. Godfrey, “Spectroscopy of  $B_c$  mesons in the relativized quark model,” *Phys. Rev. D* **70**, 054017 (2004) [hep-ph/0406228].
- [48] S. Godfrey, “Properties of the charmed P-wave mesons,” *Phys. Rev. D* **72**, 054029 (2005) [hep-ph/0508078].
- [49] M. Di Pierro and E. Eichten, “Excited heavy - light systems and hadronic transitions,” *Phys. Rev. D* **64**, 114004 (2001) [hep-ph/0104208].
- [50] D. Ebert, V. O. Galkin and R. N. Faustov, “Mass spectrum of orbitally and radially excited heavy - light mesons in the relativistic quark model,” *Phys. Rev. D* **57**, 5663 (1998) [*Phys. Rev. D* **59**, 019902 (1999)] [hep-ph/9712318].
- [51] D. Ebert, R. N. Faustov and V. O. Galkin, “Heavy-light meson spectroscopy and Regge trajectories in the relativistic quark model,” *Eur. Phys. J. C* **66**, 197 (2010) [arXiv:0910.5612 [hep-ph]].
- [52] S. F. Radford, W. W. Repko and M. J. Saelim, “Potential model calculations and predictions for  $c\bar{s}$  quarkonia,” *Phys. Rev. D* **80**, 034012 (2009) [arXiv:0903.0551 [hep-ph]].
- [53] M. Shah, B. Patel and P. C. Vinodkumar, “Mass spectra and decay properties of  $D_s$  meson in a relativistic Dirac formalism,” *Phys. Rev. D* **90**, no. 1, 014009 (2014) [arXiv:1402.4227 [hep-ph]].
- [54] S. N. Gupta and J. M. Johnson, “Quantum chromodynamic potential model for light heavy quarkonia and the heavy quark effective theory,” *Phys. Rev. D* **51**, 168 (1995) [hep-ph/9409432].
- [55] F. E. Close and E. S. Swanson, “Dynamics and decay of heavy-light hadrons,” *Phys. Rev. D* **72**, 094004 (2005) [hep-ph/0505206].
- [56] T. Barnes and S. Godfrey, “Charmonium options for the  $X(3872)$ ,” *Phys. Rev. D* **69**, 054008 (2004) [hep-ph/0311162].
- [57] T. Barnes, S. Godfrey and E. S. Swanson, “Higher charmonia,” *Phys. Rev. D* **72**, 054026 (2005) [hep-ph/0505002].
- [58] H. G. Blundell and S. Godfrey, “The  $\xi(2220)$  reexamined: Strong decays of the  $1^3F_2$  and  $1^3F_4$   $s\bar{s}$  mesons,” *Phys. Rev. D* **53**, 3700 (1996) [hep-ph/9508264].
- [59] S. Godfrey, “Testing the nature of the  $D_{sJ}^*(2317)^+$  and  $D_{sJ}(2463)^+$  states using radiative transitions,” *Phys. Lett. B* **568**, 254 (2003) [hep-ph/0305122].
- [60] B. Aubert *et al.* [BaBar Collaboration], “Observation of a narrow meson decaying to  $D_s^+ \pi^0$  at a mass of  $2.32\text{-GeV}/c^2$ ,” *Phys. Rev. Lett.* **90**, 242001 (2003) [hep-ex/0304021].
- [61] P. Krokovny *et al.* [Belle Collaboration], “Observation of the  $D_{sJ}(2317)$  and  $D_{sJ}(2457)$  in  $B$  decays,” *Phys. Rev. Lett.* **91**, 262002 (2003) [hep-ex/0308019].
- [62] S.-K. Choi *et al.* [Belle Collaboration], “Observation of a Narrow Charmoniumlike State in Exclusive  $B^\pm \rightarrow$

- $K^\pm\pi^+\pi^-J/\psi$  Decays,” Phys. Rev. Lett. **91**, 262001 (2003) [hep-ex/0309032].
- [63] S. Godfrey and S. L. Olsen, “The Exotic XYZ Charmonium-like Mesons,” Ann. Rev. Nucl. Part. Sci. **58**, 51 (2008) [arXiv:0801.3867 [hep-ph]].
- [64] S. Godfrey, “Topics in Hadron Spectroscopy in 2009,” arXiv:0910.3409 [hep-ph].
- [65] E. Braaten, “Theoretical Interpretations of the XYZ Mesons,” arXiv:1310.1636 [hep-ph].
- [66] F. De Fazio, “New Spectroscopy of Heavy Mesons,” PoS HQL **2012**, 001 (2012) [arXiv:1208.4206 [hep-ph]].
- [67] E. J. Eichten, K. Lane and C. Quigg, “Charmonium levels near threshold and the narrow state  $X(3872) \rightarrow \pi^+\pi^-J/\psi$ ,” Phys. Rev. D **69**, 094019 (2004) [hep-ph/0401210].
- [68] R. N. Cahn and J. D. Jackson, “Spin orbit and tensor forces in heavy quark light quark mesons: Implications of the new  $D_s$  state at 2.32-GeV,” Phys. Rev. D **68**, 037502 (2003) [hep-ph/0305012].
- [69] E. J. Eichten and C. Quigg, “Mesons with beauty and charm: Spectroscopy,” Phys. Rev. D **49**, 5845 (1994) [hep-ph/9402210].
- [70] This is discussed more fully in Appendix A of T. Barnes, N. Black and P. R. Page, “Strong decays of strange quarkonia,” Phys. Rev. D **68**, 054014 (2003) [arXiv:nucl-th/0208072].
- [71] See for example W. Kwong and J. L. Rosner, “D Wave Quarkonium Levels Of The Upsilon Family,” Phys. Rev. D **38**, 279 (1988).
- [72] A. J. Siebert, “Note On The Interaction Between Nuclei And Electromagnetic Radiation,” Phys. Rev. **52**, 787 (1937).
- [73] R. McClary and N. Byers, “Relativistic Effects In Heavy Quarkonium Spectroscopy,” Phys. Rev. D **28**, 1692 (1983).
- [74] P. Moxhay and J. L. Rosner, “Relativistic Corrections In Quarkonium,” Phys. Rev. D **28**, 1132 (1983).
- [75] J. D. Jackson, “Lecture on the New Particles,” in *Proceedings of the Summer Institute on Particle Physics, August 2-13, 1976*, edited by M. C. Zipf, Stanford Linear Accelerator Center Report SLAC-198, November 1977, p. 147.
- [76] V. A. Novikov, L. B. Okun, M. A. Shifman, A. I. Vainshtein, M. B. Voloshin, and V.I.Zakharov, Phys. Rept. **C41**, 1 (1978).
- [77] This expression for the decay width comes from E. Swanson, private communication.
- [78] Relativistic effects in M1 transitions are discussed in: J. S. Kang and J. Sucher, “Radiative M1 Transitions Of The Narrow Resonances,” Phys. Rev. D **18**, 2698 (1978); H. Grotch and K. J. Sebastian, “Magnetic Dipole Transitions Of Narrow Resonances,” Phys. Rev. D **25**, 2944 (1982); V. Zambetakis and N. Byers, “Magnetic Dipole Transitions In Onia,” Phys. Rev. D **28**, 2908 (1983); H. Grotch, D. A. Owen and K. J. Sebastian, “Relativistic Corrections To Radiative Transitions And Spectra Of Phys. Rev. D **30**, 1924 (1984); X. Zhang, K. J. Sebastian and H. Grotch, “M1 Decay Rates Of Heavy Quarkonia With A Nonsingular Potential,” Phys. Rev. D **44**, 1606 (1991).
- [79] E. S. Ackleh, T. Barnes and E. S. Swanson, “On the mechanism of open flavor strong decays,” Phys. Rev. D **54**, 6811 (1996) [hep-ph/9604355].
- [80] Z. F. Sun and X. Liu, “Newly observed  $D_{sJ}(3040)$  and the radial excitations of P-wave charmed-strange mesons,” Phys. Rev. D **80**, 074037 (2009) [arXiv:0909.1658 [hep-ph]].
- [81] J. Ferretti and E. Santopinto, “Open-flavor strong decays of open-charm and open-bottom mesons in the  $^3P_0$  pair-creation model,” arXiv:1506.04415 [hep-ph].
- [82] P. Colangelo, F. De Fazio, F. Giannuzzi and S. Nicotri, “New meson spectroscopy with open charm and beauty,” Phys. Rev. D **86**, 054024 (2012) [arXiv:1207.6940 [hep-ph]].
- [83] X.-H. Zhong and Q. Zhao, “Strong decays of newly observed  $D(sJ)$  states in a constituent quark model with effective Lagrangians,” Phys. Rev. D **81**, 014031 (2010) [arXiv:0911.1856 [hep-ph]].
- [84] X.-H. Zhong and Q. Zhao, “Strong decays of heavy-light mesons in a chiral quark model,” Phys. Rev. D **78**, 014029 (2008) [arXiv:0803.2102 [hep-ph]].
- [85] S. Godfrey and K. Moats, “Bottomonium Mesons and Strategies for their Observation,” Phys. Rev. D **92**, no. 5, 054034 (2015) [arXiv:1507.00024 [hep-ph]].
- [86] R. Kokoski and N. Isgur, “Meson Decays by Flux Tube Breaking,” Phys. Rev. D **35**, 907 (1987). doi:10.1103/PhysRevD.35.907
- [87] H. G. Blundell, S. Godfrey and B. Phelps, “Properties of the strange axial mesons in the relativized quark model,” Phys. Rev. D **53**, 3712 (1996) doi:10.1103/PhysRevD.53.3712 [hep-ph/9510245].
- [88] J. Ferretti and E. Santopinto, “Higher mass bottomonia,” Phys. Rev. D **90**, no. 9, 094022 (2014) doi:10.1103/PhysRevD.90.094022 [arXiv:1306.2874 [hep-ph]].
- [89] J. Segovia, D. R. Entem and E. Fernandez, “Scaling of the  $^3P_0$  strength in heavy meson decays,” Phys. Lett. B **714**, 322 (2012).
- [90] Q. F. Lü and D. M. Li, “Understanding the charmed states recently observed by the LHCb and BaBar Collaborations in the quark model,” Phys. Rev. D **90**, no. 5, 054024 (2014) [arXiv:1407.3092 [hep-ph]].
- [91] E. van Beveren and G. Rupp, “New BABAR state  $D(sJ)$  (2860) as the first radial excitation of the  $D^*(s_0)(2317)$ ,” Phys. Rev. Lett. **97**, 202001 (2006) [hep-ph/0606110].
- [92] A. Zhang, “Implications to c anti-s assignments of  $D(s_1)(2700)^+$  and  $D(sJ)(2860)$ ,” Nucl. Phys. A **856**, 88 (2011) [arXiv:0904.2453 [hep-ph]].
- [93] B. Chen, D. -X. Wang and A. Zhang, “Interpretation of  $D_{sJ}(2632)^+$ ,  $D_{s_1}(2700)^\pm$ ,  $D_{sJ}^*(2860)^+$  and  $D_{sJ}(3040)^+$ ,” Phys. Rev. D **80**, 071502 (2009) [arXiv:0908.3261 [hep-ph]].
- [94] D. -M. Li and B. Ma, “Implication of BaBar’s new data on the  $D_{s_1}(2710)$  and  $D_{sJ}(2860)$ ,” Phys. Rev. D **81**, 014021 (2010) [arXiv:0911.2906 [hep-ph]].
- [95] G. -L. Wang, Y. Jiang, T. Wang and W. -L. Ju, “The Properties of  $D_{s_1}^*(2700)^+$ ,” arXiv:1305.4756 [hep-ph].
- [96] B. Chen, X. Liu and A. Zhang, “A combined study of  $2S$  and  $1D$  open-charm mesons with natural spin-parity,” arXiv:1507.02339 [hep-ph].
- [97] X. H. Zhong, “Strong decays of the newly observed  $D(2550)$ ,  $D(2600)$ ,  $D(2750)$ , and  $D(2760)$ ,” Phys. Rev. D **82**, 114014 (2010) [arXiv:1009.0359 [hep-ph]].
- [98] L. Yuan, B. Chen and A. Zhang, “ $D_{s_1}^*(2700)^\pm$  and  $D_{sJ}^*(2860)^\pm$  Revisited within the  $^3P_0$  Model,” arXiv:1203.0370 [hep-ph].
- [99] P. Colangelo and F. De Fazio, “Open charm meson spectroscopy: Where to place the latest piece of the puzzle,”

Phys. Rev. D **81**, 094001 (2010) [arXiv:1001.1089 [hep-ph]].